Fatty acid MAMP, arachidonic acid, and brown seaweed derived biostimulant induce local and systemic overlapping transcriptional and metabolic remodeling in tomato

By

DOMONIQUE CHRISTIAN ANN LEWIS

DISSERTATION

Submitted in partial satisfaction of the requirements for the degree of

DOCTOR OF PHILOSOPHY

in

Plant Pathology

in the

OFFICE OF GRADUATE STUDIES

of the

UNIVERSITY OF CALIFORNIA

DAVIS

Approved:

Richard Bostock, Ph.D., Chair

Gitta Coaker, Ph.D.

Takao Kasuga, Ph.D.

Committee in Charge

2022

In loving memory of my ancestors, enslaved and free.

TABLE OF CONTENTS

Fatty acid MAMP, arachidonic acid, and brown seaweed derived biostimulant induce local and systemic overlapping transcriptional and metabolic remodeling in tomato

Abstract

Eicosapolyenoic fatty acids are integral components of oomycete pathogens that can act as microbe-associated molecular patterns (MAMPs) to induce disease resistance in plants. Defense inducing eicosapolyenoic fatty acids include arachidonic (AA) and eicosapentaenoic acids, and are strong elicitors in solanaceous plants with bioactivity in other plant families. Similarly, extracts of the brown seaweed, *Ascophyllum nodosum*, used in sustainable agriculture as a biostimulant of plant growth, may also induce disease resistance. *A. nodosum*, similar to other macroalgae, is rich in eicosapolyenoic fatty acids, which comprise as much as 25% of total fatty acid composition. I investigated the response of roots and leaves from AA or a commercial *A. nodosum* extract (ANE) on root-treated tomatoes via RNA sequencing, phytohormone profiling, and disease assays. AA and ANE significantly altered transcriptional profiles relative to control plants, inducing numerous defense-related genes with both substantial overlap as well as differences in gene expression patterns. Root treatment with AA and, to a lesser extent, ANE also altered both salicylic acid and jasmonic acid levels while inducing local and systemic resistance to oomycete and bacterial pathogen challenge. The transcriptomic portion of this dissertation study highlights overlap in both local and systemic defense induced by AA and ANE, with potential for inducing broad-spectrum resistance against pathogens.

Results of the conducted RNA sequencing analysis coupled with the shared induced resistance phenotype indicated that AA and ANE treatment may also elicit similar metabolic changes in tomato. In this dissertation work, untargeted metabolomic analysis via LCMS was conducted to investigate the local and systemic metabolome-wide remodeling events induced by

AA- and ANE-root treatment. This study demonstrated AA and ANE's capacity to locally and systemically alter the metabolome of tomato with enrichment of chemical classes and accumulation of metabolites associated with defense-related secondary metabolism. AA and ANE root-treated plants showed enrichment of fatty acyl-glycosides and strong modulation of hydroxycinnamic acids and derivatives. Identification of specific metabolites whose accumulation was affected by AA and ANE treatment revealed shared metabolic changes related to ligno-suberin biosynthesis and the synthesis of phenolic compounds. The metabolomics portion of this dissertation highlights the extensive local and systemic metabolic changes in tomato induced by treatment with a fatty acid MAMP and a seaweed-derived plant biostimulant with implications for induced resistance and crop improvement.

Introductory Chapter

Fatty acids are essential components of all cells and serve key structural and functional roles, with many that serve as precursors to bioactive molecules[1]. Eicosapolyenoic (EP) fatty acids, such as arachidonic acid (AA; all cis-5,8,11,14-eicosatetraenoic acid) and eicosapentaenoic acid (EPA; all cis-5,8,11,14,17-eicosapentaenoic acid), have important roles in stress signaling and immune responses that are evolutionarily conserved across kingdoms [2]. In mammalian biology, AA and EPA are oxidized to form eicosanoids, important inflammatory molecules that mediate immune responses such as fever, inflammation, allergic responses, and vasoconstriction [3, 4]. In plant-microbe interactions, AA and EPA released by pathogens can elicit host immunity and defense [2].

AA and EPA were first isolated and identified as potent elicitors of plant defense in the potato- *Phytophthora infestans* interaction. Spore and mycelial extracts from *P. infestans* applied to potato tuber discs induced phytoalexin accumulation and triggered cell death similar to the hypersensitive response associated with incompatible races of the pathogen [5]. Fractionation and analysis of mycelial and sporangial extracts elucidated AA and EPA as the simplest, most active elicitors of sesquiterpenoid phytoalexin accumulation and other defense-related responses. Treatment of tuber discs with a collection of naturally occurring saturated and unsaturated fatty acids, including the principal polyunsaturated fatty acids found in plants, linoleic acid (LA) and α-linolenic acid (ALA), showed no defense response induction [5]. Additionally, the application of AA to potato tuber discs was shown to protect against subsequent infection by compatible races of *P. infestans* [6]. Microautoradiographic analyses demonstrated the release of AA and its metabolites from *P. infestans* spores and hyphae during the infection process [7], while the metabolic fate of AA was investigated through experiments

with radiolabeled AA that demonstrated its rapid incorporation into plant lipids as well as oxidation to hydroperoxy acids and uncharacterized products [8]. Interestingly, branched β (1,3)-glucans, also derived from *P. infestans*, were shown to enhance the defense response elicited by AA [9, 10]. Although the glucans alone did not possess elicitor activity in potato, treatment of potato tuber with AA and glucans enhanced AA-induced sesquiterpene accumulation and HR-like response [9].

EP's, like AA were historically termed 'elicitors', because of their capacity to induce immune response and protect against subsequent infection. However, they nicely fit the modern term of microbe associated molecular pattern (MAMP). EP fatty acids can be considered microbe/pathogen-associated molecular patterns (M/PAMPs), although the signal-response coupling of their action in the plant likely is different from the receptor-kinase mediated coupling observed with other MAMPs [11]. MAMPs are classically defined as essential structural components of microorganism common to both pathogenic and nonpathogenic species. They are absent from hosts and thus act as triggers of defense activation through host recognition of foreign non-self components. Traditionally MAMPs also have specific structural requirements critical for their perception and activity. EP fatty acids represent conserved and essential fatty acid components found in the storage lipids, membranes and cell walls of oomycetes, where they constitute a significant percent of total fatty acid composition [12, 13]. EP fatty acid biosynthesis is absent in higher plants, and is generally restricted to animals, lower plants, primitive fungi, and various taxa within the Stramenopila, including oomycetes[14]. Additionally, specific structural requirements for fatty acid elicitor activity include a minimum chain length of 20 carbons and at least three double bonds in cis-1,4-pentadiene configuration, and unsaturation beginning at carbon 5 in the chain for maximal activity [9].

Although EP acid MAMP activity was described first in potato, their ability to induce resistance to various pathogens and trigger phytoalexin accumulation, reactive oxygen species (ROS) production, and programmed cell death (PCD) has been investigated in other plant species. Root pretreatment with AA reduced avocado seedling colonization by *P. cinnamomi* [15]. Pearl millet seedlings exhibited a systemic acquired (SAR) resistance phenotype after seeds, treated with AA or EPA, showed a greater degree of protection from infection by the downy mildew pathogen, *Sclerospora graminicola* [16]. EP acids have been used to screen for pearl millet genotypes that display a heightened response to these elicitors and a corresponding greater resistance to *S. graminicola* [17]. SAR after EP treatment has also been reported in the Solanaceae members tomato, potato, and tobacco. Tomato leaves showed local induction of an SAR marker gene in response to leaf treatment with AA [18]. The treatment of lower potato leaves with EPs protected upper leaves from *P. infestans* infection, while induced resistance to *Alternaria solani* was seen in AA-treated potato leaves accompanied by increased levels of salicylic acid (SA) and accumulation of PR-1 transcripts [19]. The treatment of lower leaves of tobacco with the elicitor protected distal upper leaves from infection with tobacco mosaic virus (TMV) [20]. Phytoalexin accumulation in response to EP treatment has been observed in various solanaceous plants including tomato, pepper, and eggplant, and in other plant species outside this family including French bean and avocado [2]. AA and its hydroperoxides elicited PCD in tomato protoplasts [21], and ROS generation has been reported in potato tuber and pepper fruit after elicitor treatment [22]. Recently Dye et. al. demonstrated that root treatment of pepper and tomato with AA induces resistance to *P. capsici,* that tomato plants respond to AA treatment with oxylipin metabolism gene induction, and induced plants are primed for a rapid lignification response at sites of pathogen attack [23, 24].

In *Arabidopsis thaliana* transformants expressing a three-gene cassette to enable production of EPs were generated. These EP plants showed enhanced resistance to infection by *Phytophthora capsici* and *Botrytis cinerea*, and were less susceptible to aphid feeding [25]. However, EP plants exhibited increased susceptibility to *Pseudomonas syringae pv. tomato* (Pst). EP plants had increased levels of jasmonic acid (JA) and JA-inducible gene expression, while reduced SA levels and SA-inducible gene expression relative to empty cassette transformed control plants. This study also demonstrated using an allene oxide synthase (AOS) mutant that, at least in Arabidopsis, AA-induced resistance was dependent on JA biosynthesis.

Treatment of plants with a proprietary extract from the brown seaweed *Ascophylum nodosum* also elicits induced resistance to plant pathogens and induction of defense marker genes and metabolites. Commercial liquid formulations of *A. nodosum* extract (ANE) contain many polyunsaturated fatty acids (PUFAs); however, EPs like AA and EPA are the predominant PUFAs present in *A. nodosum*, making up as much as 25% of the total fatty acid composition [26, 27]. Although higher plants are capable of synthesis of long-chain hydrocarbons (e.g., waxes), polyunsaturated fatty acids greater than 18 carbons generally are not present. Algal species, similar to *A. nodosum*, are capable of EP biosynthesis and belong to the same major eukaryotic kingdom, the Stramenopila, as oomycetes. Recent research showed that application of the ANE formulation results in reduced infection levels of greenhouse cucumber plants following inoculation with the fungal pathogens *Alternaria cucumerinum*, *Didymella applanata*, *Fusarium oxysporum*, and *B. cinerea* [28]. Reduced disease was positively correlated with increased transcript accumulation of several defense genes including lipoxygenase, glucanase, and chitinase, and elevated levels of phenolic compounds compared to negative controls [28]. ANE has also been shown to reduce the foliar disease severity of *Alternaria radicina* and *B.*

cinerea infection on carrot [29]. This coincided with increased activity of defense related enzymes and increased transcript abundance of pathogenesis-related protein I (PR-1), chitinase, lipid transfer protein (LTP), phenylalanine ammonia lyase (PAL), chalcone synthase (CS), non-expressing pathogenesis-related protein (NPR-1) and pathogenesis-related protein 5 (PR-5) compared with negative controls [29].

ANE is generally applied as a plant biostimulant and has been experimentally shown to improve plant growth, development, and crop yield, and to promote resistance to abiotic and biotic challenges [30]. The application of seaweed formulations as soil amendments in agriculture dates to antiquity. Some of the earliest written accounts are from ancient Rome during the latter half of the first century. Early recommendations include applying seaweed mulch to the roots of cabbage transplants in the field and amending soil around the roots of tree crops such as pomegranate and citron [31]. Seaweed preparations have been used for millennia in agriculture for their plant growth promoting properties and are utilized by both organic and conventional commercial growers in some areas. Although it is easier to rationalize ANE's plant growth promoting properties in part to increasing soil fertility, despite widespread use, the nature of ANE's active fractions and apparent capability to induce resistance remain unclear. Characterizing the biochemical and molecular basis of AA/ANE induced disease resistance could provide a foundation to optimize the use of seaweed-based biostimulants for disease management in organic and conventional production systems.

My dissertation research utilized RNA sequencing, whole plant disease assays, phytohormone profiling, and untargeted metabolomic analysis to investigate the apparent overlap in biological activity of an oomycete derived MAMP, AA, and plant biostimulant, ANE, in tomato. To test the systemicity of AA-induced resistance and establish the local or systemic

nature of ANE-induced resistance in tomato, disease assays were conducted. Root treatment with either AA or ANE locally protected tomato seedlings from Phytophthora root and crown rot caused by *P. capsici* and systemically protected distal untreated leaves from the bacterial speck pathogen, *Pseudomonas syringae* pv. *tomato* (*Pst.*).

Because of the shared induced resistance phenotype and the predominance of AA in ANE, I sought to compare the transcriptome-wide changes elicited by AA and ANE treatment compared to water control. 3' Batch tag sequencing revealed a striking level of transcriptional congruency between AA and ANE treated plants with gene ontology function analysis of the data showing enrichment and underrepresentation of similar classes of genes. AA and ANE upregulated expression of genes associated with oxylipins, immunity, and secondary metabolism. This included induction of genes in the lipoxygenase pathway, several WRKY transcription factors, genes encoding immune receptors, and genes involved in SA and JA signaling.

Results of the transcriptomic study implicated the possible role of defense-related hormones in AA- and ANE-induced resistance. The effect of AA and ANE on the accumulation of several key phytohormones in treated tomato roots was determined via LC-MS/MS. Phytohormone quantification showed that AA and ANE treatment locally and systemically alters the phytohormone profile of tomato, modulating the levels of defense associated phytohormones, including JA and SA. Although SA and JA are often framed as antagonistic, this study revealed that AA at the concentration tested can elicit accumulation of SA and JA concurrently in tomato.

The extensive overlap in the transcriptional profiles of AA- and ANE-treated plants coupled with the shared induced resistance phenotype indicated that treatment with either AA or

ANE may elicit similar metabolic remodeling events in tomato. To assess and characterize the gross metabolic changes induced by fatty acid MAMP treatment and ANE treatment, untargeted metabolomic analysis was conducted using LC-MS. AA and ANE locally and systemically alter the metabolome of treated seedlings towards defense-associated secondary metabolism. AA- and ANE-treated plants showed enrichment of similar chemical classes including fatty acyl-glycosides and strong modulation of hydroxycinnamic acids and derivatives. Likewise, examination of specific metabolites whose accumulation was most greatly affected by AA and ANE treatment revealed sharp increases in intermediates of ligno-suberin biosynthesis and the synthesis of phenolic compounds.

Collectively, the studies of this dissertation represent a comprehensive comparative transcriptomic and metabolomic analysis of AA- and ANE-induced resistance in tomato. AA and ANE induce similar yet distinct transcriptional and metabolic changes in tomato with interesting parallels and key differences to canonical MAMPs. ANE's elicitor activity appears to be conditioned in part by EPs, with additional factors in the extract that further shape the plant's transcriptional and metabolic responses. The reported findings are an important thrust forward for an understudied aspect of molecular plant-pathogen interaction with potential to guide optimization of seaweed formulations for effective and sustainable management of plant diseases.

Literature Cited

1. Mittler, R., *Oxidative stress, antioxidants and stress tolerance.* Trends in Plant Science, 2002. **7**(9): p. 405-10.

2. Robinson, S.M. and R.M. Bostock, *β-glucans and eicosapolyenoic acids as MAMPs in plant-oomycete interactions: past and present.* Frontiers in Plant Science, 2015. **5**: p. 797-797.

3. De Caterina, R. and G. Basta, *n-3 Fatty acids and the inflammatory response — biological background.* European Heart Journal Supplements, 2001. **3**: p. D42-D49.

4. Murakami, M., *Lipid mediators in life science.* Experimental Animals, 2011. **60**(1): p. 7-20.

5. Bostock, R.M., J.A. Kuc, and R.A. Laine, *Eicosapentaenoic and arachidonic acids from Phytophthora infestans elicit fungitoxic sesquiterpenes in the potato.* Science, 1981. **212**(4490): p. 67-9.

6. Bostock, R.M., R.A. Laine, and J.A. Kuć, *Factors affecting the elicitation of sesquiterpenoid phytoalexin accumulation by eicosapentaenoic and arachidonic acids in potato.* Plant Physiology 1982. **70**(5): p. 1417-24.

7. Ricker, K.E. and R.M. Bostock, *Evidence for release of the elicitor arachidonic acid and its metabolites from sporangia of Phytophthora infestans during infection of potato.* Physiological and Molecular Plant Pathology, 1992. **41**(1): p. 61-72.

8. Preisig, C.L. and J.A. Kuć, *Metabolism by potato tuber of arachidonic acid, an elicitor of hypersensitive resistance.* Physiological and Molecular Plant Pathology, 1988. **32**(1): p. 77-88.

9. Preisig, C.L. and J.A. Kuć, *Arachidonic acid-related elicitors of the hypersensitive response in potato and enhancement of their activities by glucans from Phytophthora infestans (Mont.) deBary.* Archives of Biochemistry and Biophysics, 1985. **236**(1): p. 379-89.

10. Maniara, G., R. Laine, and J. Kuć, *Oligosaccharides from Phytophthora infestans enhance the elicitation of sesquiterpenoid stress metabolites by arachidonic acid in potato.* Physiological Plant Pathology, 1984. **24**(2): p. 177-186.

11. Ngou, B.P.M., P. Ding, and J.D.G. Jones, *Thirty years of resistance: Zig-zag through the plant immune system.* Plant Cell, 2022. **34**(5): p. 1447-1478.

12. Creamer, J.R. and R.M. Bostock, *Characterization and biological activity of Phytophthora infestans phospholipids in the hypersensitive response of potato tuber.* Physiological and Molecular Plant Pathology, 1986. **28**(2): p. 215-225.

13. Walley, J.W., et al., *Fatty acids and early detection of pathogens.* Current Opinion in Plant Biology, 2013. **16**(4): p. 520-526.

14. Gellerman, J.L., et al., *Distribution of arachidonic and eicosapentaenoic acids in the lipids of mosses.* Biochimica et Biophysica Acta 1975. **388**(2): p. 277-90.

15. María Teresa, R.-C., et al., *The avocado defense compound phenol-2,4-bis (1,1-dimethylethyl) is induced by arachidonic acid and acts via the inhibition of hydrogen peroxide production by pathogens.* Physiological and Molecular Plant Pathology, 2014. **87**: p. 32-41.

16. Amruthesh, K., et al., *Unsaturated fatty acids from zoospores of Sclerospora graminicola induce resistance in pearl millet.* European Journal of Plant Pathology, 2005. **111**: p. 125-137.

17. Geetha, S., et al., *Arachidonic acid-induced hypersensitive cell death as an assay of downy mildew resistance in pearl millet.* Annals of Applied Biology, 1996. **129**(1): p. 91-96.

18. Cohen, Y., U. Gisi, and E. Mosinger, *Systemic resistance of potato plants against Phytophthora infestans induced by unsaturated fatty acids.* Physiological and Molecular Plant Pathology, 1991. **38**(4): p. 255-263.

19. Coquoz, J.L., et al., *Arachidonic acid induces local but not systemic synthesis of salicylic acid and confers systemic resistance in potato plants to Phytophthora infestans and Alternaria solani.* Phytopathology 1995. **85**: p. 1219-1224.

20. Rozhnova, N., G. Gerashchenkov, and A. Babosha, *The Effect of Arachidonic Acid and Viral Infection on the Phytohemagglutinin Activity during the Development of Tobacco Acquired Resistance.* Russian Journal of Plant Physiology, 2003. **50**: p. 661-665.

21. Knight, V.I., et al., *Hydroperoxides of fatty acids induce programmed cell death in tomato protoplasts.* Physiological and Molecular Plant Pathology, 2001. **59**(6): p. 277-286.

22. Araceli, A.C., et al., *Capsidiol production in pepper fruits (Capsicum annuum L.) induced by arachidonic acid is dependent of an oxidative burst.* Physiological and Molecular Plant Pathology, 2007. **70**(1): p. 69-76.

23. Dye, S.M. and R.M. Bostock, *Eicosapolyenoic fatty acids induce defense responses and resistance to Phytophthora capsici in tomato and pepper.* Physiological and Molecular Plant Pathology, 2021. **114**: p. 101642.

24. Dye, S.M., J. Yang, and R.M. Bostock, *Eicosapolyenoic fatty acids alter oxylipin gene expression and fatty acid hydroperoxide profiles in tomato and pepper roots.* Physiological and Molecular Plant Pathology, 2020. **109**: p. 101444.

25. Savchenko, T., et al., *Arachidonic acid: an evolutionarily conserved signaling molecule modulates plant stress signaling networks.* Plant Cell, 2010. **22**(10): p. 3193-3205.

26. Lorenzo, J.M., et al., *Proximate composition and nutritional value of three macroalgae: Ascophyllum nodosum, Fucus vesiculosus and Bifurcaria bifurcata.* Marine Drugs, 2017. **15**(11): p. 360.

27. van Ginneken, V.J., et al., *Polyunsaturated fatty acids in various macroalgal species from North Atlantic and tropical seas.* Lipids in Health and Disease, 2011. **10**: p. 104.

28. Jayaraman, J., J. Norrie, and Z. Punja, *Commercial extract from the brown seaweed Ascophyllum nodosum reduces fungal diseases in greenhouse cucumber.* Journal of Applied Phycology, 2011. **23**: p. 353-361.

29. Jayaraj, J., et al., *Seaweed extract reduces foliar fungal diseases on carrot.* Crop Protection, 2008. **27**(10): p. 1360-1366.

30. Khan, W., et al., *Seaweed Extracts as Biostimulants of Plant Growth and Development.* Journal of Plant Growth Regulation, 2009. **28**: p. 386-399.

31. Craigie, J., *Seaweed extract stimuli in plant science and agriculture.* Journal of Applied Phycology, 2010. **23**: p. 371-393.

Overlapping local and systemic defense induced by an oomycete fatty acid MAMP and brown seaweed extract in tomato

Domonique C. Lewis[1], Danielle M. Stevens[1], Holly Little[2], Gitta L. Coaker[1], and Richard M. Bostock[1*]

[1]Department of Plant Pathology, University of California, Davis, CA 95616, USA

[2]Acadian Plant Health, Acadian Seaplants Limited, Dartmouth, Nova Scotia, Canada, B3B 1X8

*Corresponding author: R.M. Bostock; E-mail: rmbostock@ucdavis.edu

Keywords: arachidonic acid, *Ascophyllum nodosum*, *Phytophthora capsici*, plant immunity, *Pseudomonas syringae* pv. *tomato*, *Solanum lycopersicum*

Funding: Research supported in part by a Gates Millenium Scholars Program fellowship and Jastro-Shields awards to DCL, United States Department of Agriculture National Institute of Food and Agriculture grant 2021-67034-35049 to DMS, an NIH grant R35GM136402 to GC, and an unrestricted gift from Acadian Seaplants LTD to RMB.

Abstract

Eicosapolyenoic fatty acids are integral components of oomycete pathogens that can act as microbe-associated molecular patterns (MAMPs) to induce disease resistance in plants. Defense inducing eicosapolyenoic fatty acids include arachidonic (AA) and eicosapentaenoic acids, and are strong elicitors in solanaceous plants with bioactivity in other plant families. Similarly, extracts of the brown seaweed, *Ascophyllum nodosum*, used in sustainable agriculture as a biostimulant of plant growth, may also induce disease resistance. *A. nodosum*, similar to other macroalgae, is rich in eicosapolyenoic fatty acids, which comprise as much as 25% of total fatty acid composition. We investigated the response of roots and leaves from AA or a commercial *A. nodosum* extract (ANE) on root-treated tomatoes via RNA sequencing, phytohormone profiling, and disease assays. AA and ANE significantly altered transcriptional profiles relative to control plants, inducing numerous defense-related genes with both substantial overlap as well as differences in gene expression patterns. Root treatment with AA and, to a lesser extent, ANE also altered both salicylic acid and jasmonic acid levels while inducing local and systemic resistance to oomycete and bacterial pathogen challenge. Thus, our study highlights overlap in both local and systemic defense induced by AA and ANE, with potential for inducing broad-spectrum resistance against pathogens.

Introduction

Members of Phaeophyta and Rhodophyta – brown and red macroalgae – contain multiple bioactive molecules and derived oligosaccharides that are known to induce defense responses in plants (Klarzynski et al., 2003; Sangha et al., 2010; Vera et al., 2011). *Ascophyllum nodosum*, a brown alga (seaweed), is a rich source of polyunsaturated fatty acids, including the

eicosapolyenoic acids arachidonic acid (AA) and eicosapentaenoic acid (EPA), which comprise as much as 25% of total fatty acid composition (Lorenzo et al., 2017; van Ginneken et al., 2011). AA and EPA are essential fatty acids found in lipids and cell walls of oomycete pathogens, are absent from higher plants, and have specific structural requirements for elicitor activity (Araceli et al., 2007; Creamer and Bostock, 1986; Gellerman et al., 1975). Algal species like *A. nodosum* belong to the same major eukaryotic lineage as oomycetes, the Stramenopila. AA and EPA are potent oomycete-derived elicitors of plant defenses, and their elicitor activity is strongly enhanced by branched β-glucan oligosaccharins (Bostock et al., 1981; Robinson and Bostock, 2015). AA, EPA and other eicosapolyenoic acids (EPs) can be considered microbe-associated molecular patterns (MAMPs), although their initial perception and signaling is likely different than canonical MAMPs directly perceived by cell surface receptors (Ngou et al., 2022). EPs are released by *Phytophthora infestans* spores and hyphae during infection of potato leaves and are taken up and incorporated into host plant cell lipids or oxidized to hydroperoxy acids and uncharacterized products (Fournier et al., 1993; Göbel et al., 2002; Göbel et al., 2001; Hwang and Hwang, 2010; Preisig and Kuć, 1988; Ricker and Bostock, 1992; Véronési et al., 1996). Representing a novel class of MAMPs, AA and EPA engage hormone-mediated immune pathways in plants (Fidantsef and Bostock, 1998; Savchenko et al., 2010).

Extracts from *A. nodosum* are used in agriculture primarily to stimulate plant growth and development, but may also increase biotic and abiotic stress tolerances (Shukla et al., 2019). There are various commercial formulations of *A. nodosum* extracts, and each is a unique proprietary mixture. When compared, these products elicit varying transcriptional outcomes in plants (Goñi et al., 2016). The commercial *A. nodosum* extract, Acadian (hereafter ANE; APH-1011-00, Acadian Seaplants, Ltd., Nova Scotia, Canada), is a biostimulant that can also protect

plants against fungal and bacterial pathogens (Ali et al., 2016; Jayaraj et al., 2008). In *Arabidopsis thaliana*, ANE induces systemic resistance to *Pseudomonas syringae* pv. *tomato* and *Sclerotinia sclerotiorum* (Subramanian et al., 2011). Studies on ANE-induced disease resistance in *A. thaliana* and tomato implicate jasmonic acid-dependent signaling, increased ROS production, induction of numerous immune response genes, and increased defense-related proteins and metabolites (Ali et al., 2016; Cook et al., 2018; Jayaraj et al., 2008; Subramanian et al., 2011). As the predominant polyunsaturated fatty acid in *A. nodosum*, AA may contribute to ANE's biological activity. The ability of these EPs to induce resistance to diverse pathogens and trigger phytoalexin accumulation, lignin, reactive oxygen species, and programmed cell death has been shown in solanaceous and other plant families (Araceli et al., 2007; Bostock et al., 1981; Cook et al., 2018; Dye, 2020; Knight et al., 2001).

Here we investigate the overlap in plant response to AA and ANE. In this study, 3' Batch Tag Sequencing (Lohman et al., 2016; Meyer et al., 2011) was used to compare and contrast AA- and ANE-induced transcriptomes locally in treated roots and systemically in leaves of root-treated tomato seedlings, revealing extensive overlap. Using disease assays with seedlings challenged with *Phytophthora capsici* and the bacterial speck pathogen, *Pseudomonas syringae* pv. *tomato* (*Pst*), we demonstrate the systemicity of AA- and ANE-induced resistance in tomato. The effect of AA and ANE root treatments on levels of selected phytohormones in roots and leaves also were determined to establish the relationship between transcriptional reprogramming and phytohormone changes that may prime or influence host defense.

Results

Transcriptomic analyses of AA- and ANE-induced plants

We hypothesized that AA- and ANE-induced resistance may be mediated by similar or shared transcriptional changes locally, in treated roots, and systemically, in leaves of root-treated tomato seedlings. To investigate transcriptomes of AA- and ANE-treated tomato (*Solanum lycopersicum cv.* 'New Yorker'), roots of hydroponically grown seedlings were treated with 10 µM AA, 0.4 % ANE, 10 µM linoleic acid (LA), or H_2O for 6, 24, and 48 hours prior to harvest and processing for RNA sequencing (**Fig. 1A**). Water and LA, an abundant fatty acid in plants, were included as negative controls. Of the sequencing reads across all samples, 65.3%-85.7% uniquely mapped to the tomato reference genome build SL 3.0 (**Sup. Fig 1**). Principle component analysis (PCA) of normalized read count data revealed distinct clustering of treatment groups across all tested timepoints in root tissue (**Fig. 1B-1D**). Both AA and ANE treatments exhibited unique clusters whereas control treatments, H_2O and LA, clustered together at 6, 24 and 48 hours in roots. PCAs of read count data for leaf tissue showed similar but less distinct clustering across treatments and timepoints reflective of distal tissue (**Sup. Fig 2**). The most distinct clustering in leaves was observed at 24 hours where both negative controls, H_2O and LA, overlapped. Partial overlap between AA and ANE treatment groups was also observed at 24 hours in leaf tissue. Similarly, heatmaps visualizing normalized read counts of the most differentially expressed (DE) genes by fold change at 24 hours showed distinct clustering by treatment group in both roots (**Fig. 2A**) and leaves (**Fig. 2B**). DE genes were set at an absolute fold change cut-off >4 and >2 for roots and leaves respectively with adjusted p-values < 0.05 across all timepoints and treatments. Heatmaps of transcriptomes depict clear grouping of profiles across both sampled tissues. Gene expression profiles of H_2O and LA treatments were nearly indistinguishable but clearly distinct from the profiles resulting from AA and ANE treatments (**Fig. 1, Fig. 2**). AA and ANE induced robust transcriptional changes relative to

control treatments (**Fig. 1, Fig. 2**), with both elicitors effecting significant overlap in gene expression profiles, as well as notable differences between treatments.

Root treatment with AA and ANE induced transcriptional changes relative to the H_2O control both locally (roots) and systemically (leaves) with varying temporal dynamics. In AA-treated plants, transcriptional reprogramming occurred most strongly at 24 hours in roots and leaves (**Fig. 3A**). ANE-treated plants showed transcriptional changes most strongly at 6 hours in roots, and 24 hours in leaves (**Fig. 3A, Sup. Fig. 3**). Roots and leaves of either AA- or ANE-root-treated tomato seedlings have many shared DE genes, with AA-treated plants exhibiting the most numerous changes in gene expression. Within a tissue, roots and leaves shared up- and down-regulated DE genes for both AA and ANE treatments, with roots showing more DE genes than leaves (516 induced and 350 suppressed genes at 24 hours; **Fig. 3C**). By comparison, leaves had 51 induced and 77 suppressed genes at 24 hours (**Sup. Fig. 3**).

Although AA and ANE root treatments altered expression of many of the same genes, these treatments also induced distinct transcriptome features in roots and leaves. Of genes that were unique to each treatment, roots displayed a higher number of these features with 1585 genes identified compared to 263 genes in leaves (**Fig. 3C**). At the earliest tested timepoint, the transcriptional profile of ANE-treated roots revealed more than 76% unique DE genes. At 24- and 48-hour time points, AA- and ANE-treated roots showed the most overlap in transcriptional changes with some 992 and 728 shared DE genes, respectively. Analysis of distal untreated leaf tissue also revealed a similar trend with overlap in shared DE genes occurring most robustly at 24 and 48 hours (**Sup. Fig. 3D**). Distinct transcriptional features in the leaves of AA and ANE root-treated plants can be seen across all tested timepoints with more than 61% and 45% of identified DE genes being specific to their respective treatment group at 24 hours (**Sup. Fig. 3**).

AA and ANE treatment induce upregulation of transcripts involved in oxylipins, immunity, and secondary metabolism

In order to identify specific gene categories and biological processes altered by AA and ANE treatments, we performed gene ontology (GO) functional analyses. GO analyses revealed AA and ANE root treatments enrich similar categories of tomato genes in both molecular function and biological processes categories **(Fig. 4A-4B)**. AA and ANE enriched root transcripts associated with oxidation-reduction processes, including hydrogen peroxide catabolism, oxidative stress responses, and heme binding. Both treatments induced cell wall macromolecule catabolism genes, as well as a variety of genes classically associated with defense responses.

Identification of specific defense- and stress-related genes significantly induced in AA- and ANE-treated roots at 24 hours revealed insightful overlap (**Fig. 7**). Transcripts of several key genes in biosynthesis of plant oxylipins including *α-DOX1*, *9-DES*, *9-LOX*, and *AOS3* were significantly up-regulated in response to AA and ANE root treatment. This corresponds with early work that first implicated oxylipin metabolism in AA action and demonstrated the capacity of plant endogenous *9-LOX* to use AA as a substrate (Andreou et al., 2009; Fournier et al., 1993; Göbel et al., 2002; Göbel et al., 2001; Hwang and Hwang, 2010; Véronési et al., 1996). The phytohormone jasmonic acid (JA) and related metabolites are also oxylipins (Dave and Graham, 2012). We observed induction of multiple JA-responsive genes including *JA2*, *JA2L*, *JAZ11*, and *JAZ7*, which previous studies reported induction in response to *Pst* infection or exogenous application of various phytohormones (Chini et al., 2017; Du et al., 2014; Ishiga et al., 2013).

AA and ANE similarly induced genes encoding known immune signaling components in roots at 24 hours. Significant increase in expression was seen in genes encoding MAPKKK's

and several WRKY transcription factors, including *WRKY39*, which confers enhanced resistance to biotic and abiotic stressors upon overexpression in transgenic tomato (Sun et al., 2015). Accumulation of salicylic acid (SA) and induction of SA-responsive genes are hallmarks of plant immune responses, including MAMP perception (Chen et al., 2017; Tsuda et al., 2009). In roots at 24 hours we observed upregulation of *NPR1* (**Fig. 7**), encoding a SA receptor that positively regulates expression of SA-dependent genes and is considered a master regulator of SA signaling (Chen et al., 2017). Likewise, the SA marker and pathogenesis-related (PR) gene *PR-1* showed induction in roots at 24 hours. Shared concurrent induction of these immunity related genes indicate plants exposed to AA and ANE are generally primed for defense against wide array of potential pathogen challenge.

Genes involved in secondary metabolism also showed strong induction in roots at 24 hours. Shikimate pathway members phenylalanine ammonia-lyase (*PAL*) and chorismate synthase, *CS1*, had increased expression compared to water in AA- and ANE-treated roots. Up-regulation of genes involved in metabolism of other phenolic compounds included tyramine n-hydroxycinnamoyl transferase (*THT1-3*) and a polyphenol oxidase. The sesquiterpenoid biosynthesis gene viridiflorene synthase, *TSP31*, showed significant induction with an increase in $\log_2$ fold change of 9.29 and 5.66 for AA and ANE, respectively, compared to water. Genes for key early steps in terpenoid biosynthesis, 3-hydroxy-3-methylglutaryl coenzyme A synthase (*HMGCS*) and 3-hydroxy-3-methylglutaryl coenzyme A reductase 2 (*HMGCR2*), a pathogen- and elicitor-responsive isoform, showed robust increases in expression in both treatment groups (Choi et al., 1992; Stermer and Bostock, 1987).

To assess global trends in transcriptional remodeling, GO functional analyses of AA- and ANE-treated tomato revealed significant congruency in under-represented gene categories.

Nearly perfect overlap was seen in all unenriched GO terms in molecular function, biological process, and cellular compartment in roots at 24 hours (**Sup. Table 1**). Examination of specific shared genes most strongly down-regulated in response to AA and ANE treatment revealed suppression of genes associated with metal transport (**Sup. Table 2**). This included genes annotated to operate as metal, iron-regulated and copper transporters and metal tolerance in roots at 24 hours. The uptake and translocation of nutrient metals is essential for plant growth and development (Jogawat et al., 2021). The down-regulation of these transporters may indicate a shift toward defense rather than growth in the plant.

Transcriptional changes specific to AA and to ANE treatments

Considering the difference in composition of AA and ANE, we examined the strongest uniquely up- and down-regulated genes in roots at 24 hours (**Sup. Table 3**). Unique transcriptional responses for AA-treated plants revealed differential expression of ethylene and terpene biosynthesis genes and modulation of genes involved in auxin signaling, cell wall anabolism, and signaling peptide formation. This included significant induction of 1-aminocyclopropane-1-carboxylate synthase 2 (*ACS2*), and suppression of an *ACO* isoform encoding 1-aminocyclopropane-1-carboxylate oxidase-like protein. Unique up regulation was also seen in a purported sesquiterpene synthase gene that showed a $\log_2$ fold change of 5.02 compared to H_2O. Unique differential gene expression after AA treatment was also observed in small auxin up-regulated *RNA 36* (*SAUR36*) and a gene encoding a purported auxin efflux carrier. AA-treated plants showed induction of *PKS3L* which encodes a precursor of the immune signaling peptide, phytosulfokine (PKS), a recently classified damage associated molecular pattern (Zhang et al., 2018).

Unique transcriptional responses for ANE-treated roots at 24 hours include those involved in auxin signaling, cytokinin biosynthesis, specialized plant metabolism, cell proliferation, and induced resistance. This included robust induction of *SAR8.2*, encoding a systemic acquired resistance protein, and *CKX2*, encoding cytokinin oxidase 2. Significant induction was also observed for *IAA2*, an auxin regulated transcription factor. ANE-treated plants also showed up-regulation of *TCMP-1*, a tomato metallocarboxypeptidase inhibitor. Modulation was also seen in two 2-oxoglutarate and Fe(II)-dependent oxygenase superfamily members (*2ODD*s).
These data collectively show AA and ANE locally and systemically alter the transcriptional profile of tomato through modulation of many defense-related genes.

Phytohormone Quantification

AA and ANE modulate expression of genes associated with JA, SA, and ethylene phytohormone signaling and biosynthesis. Therefore, levels of selected phytohormones and phytohormone precursors were quantified via LC-MS/MS (**Fig. 5**). The JA precursor, oxophytodienoic acid (OPDA), accumulated in the leaves of AA- and ANE-root-treated plants at 48 hours, while accumulation of JA and its isoleucine conjugate (JA-Ile) occurred in the roots of AA-treated roots at 24 hours. This coincides with induction of JA signaling components *JA2*, *JA2L*, *JAZ7*, and *JAZ11* in the roots of AA-treated plants at 24 hours (**Fig. 7**). Salicylic acid (SA) accumulated in roots of AA-treated plants at both sample time points, consistent with our observation of transcriptional upregulation of *NPR1* and *PR1* (**Fig. 7**). Elevated levels of SA also were seen in leaves of both AA- and ANE-root-treated seedlings at 48 hours. Abscisic acid (ABA) increased in leaf tissue 24 and 48 hours after root treatment with AA or ANE. Indole acetic acid (IAA) and its aspartate conjugate (IAA-Asp) and zeatin riboside isomers were reduced at 24 hours in the

roots of both AA- and ANE-treated plants. These changes in accumulation of IAA and its conjugate are consistent with the unique differential gene expression in small auxin up-regulated *RNA 36* (*SAUR36*) and a gene encoding a purported auxin efflux carrier in AA-treated roots at 24 hours. Likewise altered levels of IAA/IAA-Asp also coincide with the unique induction of *IAA2*, an auxin-regulated transcription factor, in the roots of ANE-treated plants at 24 hours. The leaves of AA- and ANE-root-treated plants also had reduced levels of zeatin ribosides at 24 and 48 hours. Taken together, these data demonstrate that AA and ANE both alter the accumulation of multiple phytohormones, including those that modulate defense networks in tomato.

Local and systemic induced resistance

Given the overlapping transcriptional profiles and clear changes in phytohormone accumulation induced by AA and ANE root treatment, we utilized disease assays to establish the systemic nature of AA-induced resistance and to investigate the local and systemic nature of ANE-induced resistance. AA-, ANE-, or H_2O-pretreated roots were inoculated with zoospores of the oomycete *P. capsici* and then seedlings were evaluated for collapse due to root and crown rot. Post-inoculation, 85% of plants treated with H_2O collapsed at the crown while less than 20% of ANE-treated plants collapsed. Treatment of roots with 0.4% ANE protected seedlings against *Phytophthora* root and crown rot compared to H_2O-treated/inoculated control seedlings (**Fig. 6A and C**). ANE's level of protection is similar to that observed with AA-induced resistance in tomato and pepper to *P. capsici* infection using this same assay format (Dye and Bostock, 2021).

The leaves of plants with roots treated with AA, ANE, or H_2O were challenged with the bacterial pathogen *Pst*. Both AA- and ANE-root treatments induced systemic resistance to *Pst*. The leaves of seedlings that had been root-treated with either AA or ANE showed significantly

reduced bacterial colonization 72 hpi compared to H_2O-treated/inoculated control seedlings (**Fig. 6B**), with leaf symptoms corresponding to treatment effects on colonization (**Fig. 6E**). H_2O control plants showed an average bacterial titer of 7.06 log CFU/cm^2, with AA- and ANE-treated plants showing a 1.25- and 1.35-fold decrease in bacterial growth, respectively. The observed leaf symptoms 72 hpi were also consistent with differences in bacterial colonization. These experiments demonstrate that both AA and ANE induced local and systemic resistance to subsequent infection with an oomycete pathogen after root inoculation or a bacterial pathogen after leaf inoculation.

Direct effect of ANE on plant growth and zoospore motility

A tradeoff often occurs between plant growth and defense, which is frequently observed in seedlings after treatment with high concentrations of MAMPs, resulting in seedling growth inhibition (Gómez-Gómez et al., 1999). Therefore, we investigated the effect of ANE on plant growth in a hydroponic system. Direct treatment of tomato roots with 0.4% ANE significantly reduced fresh weight biomass compared to water at 72 hours post treatment, consistent with an ANE-associated growth penalty (**Sup. Fig. 4A**). The ANE growth penalty is observed locally in treated roots (**Sup. Fig. 4B**) and distally in shoots (**Sup. Fig. 4C**), consistent with ANE's ability to systemically alter the transcriptional profile and induce resistance.

Typically, MAMPs are thought to primarily act to inhibit pathogen proliferation through direct perception and defense activation in the plant. However, ANE is a complex mixture with many potentially bioactive compounds. Because a potential direct effect of ANE on zoospores of *Phytophthora* has not been reported, we investigated ANE's effect on zoospore integrity and encystment. In a concentration-dependent manner, zoospores of *P. capsici* encyst and lyse in the

presence of ANE (**Fig. 6D**). Zoospores exposed to dilute ANE (≤ 0.1%) showed abnormal motility or premature encystment compared to water controls, while zoospores treated with ≥ 0.3% ANE showed premature enystment and lysis compared to water controls (**Sup. Table 4**). These data demonstrate ANE's ability to alter zoospore motility by inducing abnormal movement, encystment, and lysis. Therefore, components in ANE not only trigger defense in tomato, but have the capacity to affect *P. capsici* zoospore behavior and viability following direct exposure**.**

Discussion

AA and related eicosapolyenoic fatty acids are unusual elicitors of defense whose structural requirements for activity, absence from higher plants, and abundance in oomycete pathogens distinguish them as MAMPs (Robinson and Bostock, 2015). *A. nodosum*, the brown alga from which ANE is derived, belongs to the same major lineage as oomycetes and contains AA as a predominant polyunsaturated fatty acid (van Ginneken et al., 2011). ANE is used commercially in crops as a biostimulant and may also help plants cope with biotic and abiotic stresses. Through comparative transcriptomic analysis, our study revealed that root treatment with AA or ANE locally and systemically induce similar yet distinct transcriptional profiles in tomato. Root treatment with AA or ANE alter the accumulation of defense-related phytohormones locally in treated roots and systemically in untreated leaves. This study also revealed the systemic nature of AA-induced resistance, and the local and systemic nature of ANE-induced resistance in tomato against pathogens with different parasitic strategies.

Unlike canonical MAMPs that are perceived at the cell surface, AA is rapidly taken up by plant cells and metabolized, with significant incorporation into plant lipids (Preisig and Kuć,

1988; Ricker and Bostock, 1992). Therefore, perception of AA, and by inference the AA present in ANE, is likely different or more complex than direct immune-receptor mediated MAMP recognition and signal transduction. AA can directly engage endogenous plant oxylipin metabolism via action of specific lipoxygenases (LOX) that use AA as a substrate (Andreou et al., 2009; Fournier et al., 1993; Göbel et al., 2002; Göbel et al., 2001; Hwang and Hwang, 2010; Véronési et al., 1996). This study demonstrates AA and ANE induce multiple overlapping local and systemic responses, with interesting parallels and key differences with canonical MAMPs.

AA and ANE locally and systemically alter transcriptional profiles of tomato with many shared and unique features. Varying levels of transcriptional overlap were seen across time points and tissues with up to 80% overlap in roots and up to 55% overlap in leaves between genes differentially expressed compared to water in AA- and ANE-treated plants (**Fig. 3C-D**). Similarly, the canonical MAMPs elf18 and flg22 induce distinct yet primarily overlapping transcriptional changes in *A. thaliana* (Wan et al., 2019). More recent work in *A. thaliana* compared the early transcriptional response of plants treated with diverse MAMPs and damage associated molecular patterns (DAMPs), which elicited striking levels of transcriptional congruency at early time points (5 min to 3 hours) (Bjornson et al., 2021). Like traditional MAMPs, AA and ANE also induce expression of genes associated with PTI including several *WRKY* transcription factors and SA receptor *NPR1*, which also accumulates in response to flg22 treatment in *A. thaliana* (Bjornson et al., 2021; Chen et al., 2017). Despite being an "orphaned" MAMP that may have a different mode of perception, AA and by inference ANE still engage common transcriptional and hormone-mediated defenses.

Systemic resistance is often induced in plants treated with MAMPs and thus is considered a product of the immune response (Mishina and Zeier, 2007). Root treatment with either AA or

ANE protected plants locally from *P. capsici*, and systemically from *Pst*. MAMP treatment is also commonly associated with plant growth inhibition due to a growth vs. defense tradeoff (Wang and Wang, 2014). As plants prime defense, there can be down-regulation of photosynthesis-related genes and a shift of photoassimilate from growth to defense, resulting in a growth penalty. Flg22 and elf18 treatment of *A. thaliana* inhibits seedling growth (Gómez-Gómez et al., 1999). Likewise, AA at concentrations used to induce immunity can significantly reduce tomato seedling length and inhibit lateral root formation and cotyledon expansion (Dye and Bostock, 2021). We found that tomato roots treated with 0.4% ANE in a hydroponic system display a significant reduction in root and shoot fresh weight (**Sup. Fig 3**). Our findings coincide with a systemic induced resistance phenotype and growth penalty associated with other well-characterized MAMPs.

Although there is striking overlap between AA/ANE and some MAMP-induced immune responses, there are also distinct differences in how AA/ANE potentially interact with immune signaling and defense. A previous gene expression study in tomato revealed AA-root treatment strongly induces local and systemic expression of several key oxylipin pathway genes (Dye, 2020). Here we show upregulation of the same subset of genes in response to ANE root treatment. Like AA, ANE also activates expression of *α-DOX1* and *9-LOX*, both of which form fatty acid hydroperoxides representing a first step in the generation of plant oxylipins. Oxylipins can serve as signaling molecules to mediate plant responses to wounding, abiotic stress, and pathogen attack (Robinson and Bostock, 2015). As with AA, ANE also induces expression of 9-DES, which can produce novel antimicrobial divinyl ethers that may operate to help restrict *Phytophthora* infections (Weber et al., 1999). Orthologs of *9-LOX* and *9-DES* are present in pepper, potato, and tobacco, and the 9-LOXs in these species can use AA as a substrate (Andreou

et al., 2009; Fournier et al., 1993; Göbel et al., 2002; Göbel et al., 2001; Hwang and Hwang, 2010; Véronési et al., 1996). Like AA, ANE induces expression of AOS3, which produces unstable allene oxides from 13-hydroperoxy fatty acids, the first committed step in JA biosynthesis. Previous work with an *aos* mutant in *A. thaliana* established that an intact JA pathway was required for AA-induced resistance to *Botrytis cinerea* (Savchenko et al., 2010). The same study showed that AA treatment of *Arabidopsis* and tomato leaves increased JA and reduced SA levels in the plants, a treatment effect abolished in the case of the *Arabidopsis aos* mutant. These data highlight the critical role of oxylipin metabolism and potentially of oxidized products of AA to help trigger changes in defense hormone signaling.

In the present study, we found accumulation of OPDA, JA, and SA concurrently in AA- and ANE-root treated tomato plants with an induced resistance phenotype. Similarly, Lal et al found that *A. thaliana* with phosphomimetic mutations in receptor-like kinase, BIK1, displayed elevated levels of both SA and JA in noninfected and in *Pst*-challenged plants (Lal et al., 2018). Our data suggest that modulation of JA and SA, classically antagonistic in induced resistance studies, is complex and nuanced in tomato in response to AA and ANE. These findings also suggest that AA and ANE can induce broad-spectrum resistance to pathogens that utilize different parasitic strategies.

While AA and ANE treatment have similar transcriptional outcomes *in planta* and share ability to induce local and systemic resistance, ANE is a complex extract containing EP as well as additional potentially bioactive compounds. Early work with AA demonstrated that it has no direct effect on zoospore motility or viability of *P. infestans* and *P. capsici* (Ricker and Bostock, 1994). In contrast, we found that direct exposure of *P. capsici* zoospores to ANE diminishes motility and viability in a concentration-dependent manner (**Sup. Fig 4, Supp. Table 4**).

However, our induced resistance experimental format with *P. capsici* ensured that zoospores did not come into direct contact with inhibitory concentrations of ANE. Also, the relevance of our observation in field settings is unclear since we would expect there to be substantial dilution of ANE during soil applications. Nonetheless, the potential to directly inhibit pathogen inoculum should be considered in experimental design in assessments of seaweed-derived and other biostimulants.

This study provides in-depth profiles of AA- and ANE-associated local and systemic transcriptional remodeling events, phytohormone changes, and induced resistance in tomato with interesting parallels and differences with canonical MAMP action. Further investigation and functional analyses of oxylipin metabolism genes in relation to AA/ANE action is needed to help elucidate their potential role in MAMP signaling. Future research with EP-containing biostimulants will lead to a more holistic understanding of diverse MAMP perception and response, with potential practical implications for crop disease management.

Materials and Methods

Disease and plant growth assays

Plant Materials and hydroponic growth system

Seeds of tomato (*Solanum lycopersicum cv.* 'New Yorker') were surface sterilized and germinated for 10 days on germination paper. Seedlings were transferred to a hydroponic growth system and maintained in a growth chamber as previously described in (Dye, 2020). Seed was obtained from a commercial source (Totally Tomatoes, Randolph, WI).

Root treatments

Fatty acid sodium salts (Na-FA; Nu-Chek Prep, Elysian, MN) were prepared and stored as previously described (Dye, 2020). A proprietary formulation of *A. nodosum* extract (ANE; APH-1011-00, Acadian Seaplants, Ltd, Nova Scotia, Canada) was diluted with deionized water (diH_2O) to a 10% working concentration, which was used to prepare treatment dilutions. All chemicals were diluted to their treatment concentrations with sterile diH_2O. Hydroponically reared, 3-week-old tomato seedlings with two fully expanded true leaves were transferred to 1 L darkened treatment containers. For *P. capsici* disease assays and ANE growth penalty assessments, roots were treated with an aerated 0.4% ANE solution, or sterile diH_2O (control) for 72 hours. For *Pst* disease assays, roots were treated with an aerated suspension of 10 µM Na-AA, 0.4% ANE, or diH_2O for 72 hours. Roots were soaked and rinsed as previously described (Dye and Bostock, 2021). Treated seedlings were then returned to treatment containers with aerated 0.5X Hoagland's solution for 72 hours followed by harvest for biomass measurements or inoculation with either *P. capsici* or *Pst*.

Phytophthora capsici root inoculation and disease assessment

For root/crown disease assays, *P. capsici* isolate PWB-53 (Hensel) was used for inoculation. Tomato seedlings were individually inoculated with 5 mL of zoospore suspension ($0.5x10^4$ per mL) as described in (Dye, 2020). Seventy-two hours post inoculation (hpi), disease incidence was rated on the basis of seedling collapse at the crown. Pathogen cultures were maintained, inoculum prepared, and seedling collapse determined as previously described (Dileo et al., 2010; Dye, 2020; Dye and Bostock, 2021).

Pst inoculation and analysis of bacterial growth

For leaf disease assays, *Pst* strain DC3000 was used for inoculation. *Pst* from -80°C-maintained glycerol stock was grown on NYGA media amended with rifampicin at 100 µg/mL for two days at 28°C. *Pst* was restreaked on rifampicin-amended NYGA media and grown for 24 hours at 28°C. The bacteria were harvested and resuspended in 5 mM $MgCl_2$. Leaves were sprayed with bacterial suspension of $OD^{600} = 0.3$ with 0.01% Silwett using a Preval spray system, Nokoma Products, Bridgefield, IL). Plants were sprayed until runoff with abaxial and adaxial leaf surfaces covered. Cut Parafilm was used as a protective barrier around the base of plants to prevent contamination of the hydroponic system. Plants were covered with clear plastic bags for 48 hpi. Bacterial colonization was quantified by growth curve analysis 4 days post-inoculation (dpi) as described by (Liu et al., 2009).

ANE growth penalty assay

Post treatment and Hoagland's solution interval, tomato seedling were harvested and roots excised from shoots. Root and shoot tissue samples were individually weighed and fresh weights recorded. Roots represent all below surface plant tissue beneath the hypocotyl and shoots represent all aerial tissue including leaves.

3'Batch Tag Sequencing Assay

Root treatment, tissue harvest, and RNA Extraction

For tissue samples for 3' Batch Tag Sequencing, roots were treated with an aerated solution of 10µM AA, 10µM LA, 0.4% Acadian, or diH_2O. Harvested tissue was then subjected to total RNA extraction using Qiagen's RNeasy Plant Mini Kit, with off column DNase digestion using

Qiagen's RNase-Free DNase Set (Qiagen, Germantown, MD). Each sample was the pool of roots or leaves of two seedlings with three replications per tissue, treatment, and timepoint. All samples were then submitted to the UC Davis Genome Center's DNA Technology Core for quality control via bioanalyzer analysis, RNA-seq library generation, and sequencing. Gene expression profiling was carried out using a 3'-Tag-RNA-Seq protocol. Barcoded sequencing libraries were prepared using the QuantSeq FWD kit (Lexogen, Vienna, Austria) for multiplexed sequencing according to the recommendations of the manufacturer using both the UDI-adapter and UMI Second-Strand Synthesis modules (Lexogen). The fragment size distribution of the libraries was verified via micro-capillary gel electrophoresis on a LabChip GX system (PerkinElmer, Waltham, MA). The libraries were quantified by fluorometry on a Qubit fluorometer (LifeTechnologies, Carlsbad, CA), and pooled in equimolar ratios. The library pool was Exonuclease VII (NEB, Ipswich, MA) treated, SPRI-bead purified with KapaPure beads (Kapa Biosystems / Roche, Basel, Switzerland), and quantified via qPCR with a Kapa Library Quant kit (Kapa Biosystems) on a QuantStudio 5 RT-PCR system (Applied Biosystems, Foster City, CA). Up to forty-eight libraries were sequenced per lane on a HiSeq 4000 sequencer (Illumina, San Diego, CA) with single-end 100 bp reads.

RNAseq data processing and analysis

The raw reads were imported into the Galaxy platform for comprehensive data analysis including quality control, alignment, and differential expression analysis (Goecks et al., 2010). The raw data was processed using the quality control tool FastQC/MultiQC (v1.7) to access the quality of the raw sequence data (Ewels et al., 2016). Read alignment was conducted using RNA STAR aligner (v2.6.0b-1) and post alignment quality control employed FastQC/MultiQC (v1.7) (Ewels

et al., 2016). Quantification of reads per gene was carried out using featureCounts (v1.6.3) (Liao et al., 2013). Read counts were normalized and differential gene expression analysis conducted using DESeq2 (v2.11.40.6) (Love et al., 2014). Differential genes were visualized using the Heatmap2 (v1.0) program followed by functional enrichment of differential genes by the program GoSeq (1.34.0) (Young et al., 2010). All aforementioned bioinformatics programs were accessed through the Galaxy toolshed (Blankenberg et al., 2014). Differential gene expression was also visualized as volcano plots developed using ggplot2 (v3.3.5) via a custom script (Supplemental_File_1).

Phytohormone quantitation

For phytohormone quantitation, roots were treated with an aerated suspension of 10 μM Na-AA (in deionized water), 0.4% ANE (in deionized water), or deionized water. Following 24- and 48-hours root exposure to their respective treatments, plants were harvested, root and leaf tissue dissected from shoots, and the collected tissue flash frozen in liquid nitrogen. Root and leaf tissue samples were submitted to the Donald Danforth Plant Science Center's Proteomics and Mass Spectrometry Facility for acidic plant hormone extraction and quantification. Each sample was the pool of roots and leaves of three seedlings with three samples per tissue, treatment, and timepoint. The experiment was performed once.

Analytical reference standards were used for the following analytes: indole-3-acetic acid (IAA; Sigma-Aldrich St. Louis, MO), N-(3-indolylacetyl)-DL-aspartic acid (IAA-Asp; Sigma-Aldrich, St. Louis, MO), (+/-)-jasmonic acid (JA; Tokyo Chemical Industry Company, Tokyo, Japan), salicylic acid (SA; Acros Organics, Geel, Belgium), (+/-)-abscisic acid (ABA; Sigma-Aldrich, St. Louis, MO), N-jasmonyl-L-isoleucine (JA-Ile; Toronto Research Chemicals,

Toronto, ON), 12-oxo-phytodienoic acid (OPDA; Cayman Chemical, Kalamazoo, MI), *cis*-zeatin (*c*Z; Santa Cruz Biotechnology, Santa Cruz, CA), *trans*-zeatin (*t*Z; Caisson Labs, Smithfield, UT), DL-dihydrozeatin (DHZ; Research Products International, Mount Prospect, IL), and *trans*-zeatin riboside (*t*ZR; Gold Biotechnology, St. Louis, MO). Internal standards were d_5-JA (Tokyo Chemical Industry Company, Tokyo, Japan), d_5-IAA (CDN Isotopes, Pointe-Claire, QC), d_5-dinor-OPDA (Cayman Chemical, Kalamazoo, MI), d_6-SA(CDN Isotopes, Pointe-Claire, QC), d_6-ABA (ICON Isotopes, Dexter, MI), d_5-*trans*-zeatin (OlChemIm, Olomouc, Czech Republic), d_5-*trans*-zeatin riboside (OlChemIm, Olomouc, Czech Republic), $^{13}C_6{}^{15}N$ JA-Ile (New England Peptide, Gardner, MA), and $^{13}C_4{}^{15}N$ IAA-Asp (New England Peptide, Gardner, MA). LC-MS grade methanol (MeOH) and acetonitrile (ACN) were sourced from J.T. Baker (Avantor Performance Materials, Radnor, PA) and LC-MS grade water was purchased from Honeywell Research Chemicals (Mexico City, Mexico). Standard and internal standard stock solutions were prepared in 50% methanol and stored at -80° C. Calibration standard solutions were prepared fresh in 30% methanol.

Phytohormone Extraction

Phytohormones *c*/*t*Z, DHZ, *t*ZR, SA, ABA, IAA, IAA-Asp, JA, JA-Ile and OPDA were extracted at a tissue concentration of 100 mg/mL in ice cold 1:1 MeOH: ACN. Around 100 mg of tissue sample were weighed and 10 µL of mixed stable-isotope labeled standards (1.0 µM for d_5-*t*Z and d_5-*t*ZR, 2.5 µM for d_4-SA, d_6-ABA, d_5-JA, d5-IAA, $^{13}C_6{}^{15}N$-IAA-Asp and d5-dinor-OPDA, and 25.0 µM for $^{13}C_6{}^{15}N$-JA-Ile) were added to each sample prior to extraction. The samples were homogenized with a TissueLyzer-II (Qiagen) for 5 minutes at 15 Hz and then centrifuged at 16,000 x g for 5 minutes at 4° C. The supernatants were transferred to new 2 mL

tubes and the pellets were re-extracted with 600 µL 1:1 ice cold MeOH: ACN. These extracts were combined and dried in a vacuum centrifuge. The samples were then reconstituted in 100 µL 30% methanol, centrifuged to remove particulates, and then passed through a 0.8 µm polyethersulfone spin filter (Sartorius, Stonehouse, UK) prior to dispensing into HPLC vials for LC-MS/MS analysis.

LC-MS/MS Analysis

Phytohormones *c*/*t*Z, DHZ, *t*ZR, SA, ABA, IAA, IAA-Asp, JA, JA-Ile and OPDA were quantified using a targeted multiple reaction monitoring (MRM)/isotope dilution-based LC-MS/MS method. A Shimadzu Prominence-XR UFLC (UPLC) system connected to a SCIEX hybrid triple quadrupole-linear ion trap MS equipped with Turbo V™ electrospray ionization (ESI) source (SCIEX, Framingham, MA) were used for the quantitative analysis. Ten microliters of the reconstituted samples were loaded onto a 3.0 x 100 mm 1.8 µm ZORBAX Eclipse XDB-C_{18} column (Agilent Technologies, Santa Clara, CA, USA) and the phytohormones were eluted within 22.0 minutes, in a binary gradient of 0.1% acetic acid in water (mobile phase A) and 0.1% acetic acid in 3:1 ACN:MeOH (mobile phase B). The initial condition of the gradient was 5% B from 0 to 2.0 minutes, ramped to 40% B at 10.0 minutes, further ramped to 50%B at 15.0 minutes, and then quickly raised to 95% B at 19.0 minutes and kept at 95% B until 22.0 minutes. The flow rate was set at 0.4 mL/min. Source parameters were set as follows: curtain gas 25 psi; source gas 140 psi; source gas 250 psi; collisionally activated dissociation (CAD) gas set to 'medium'; interface heater temperature 500˚C; ion spray voltage set to +5500 V for positive ion mode and -4500 V for negative ion mode. Individual analyte and internal standard ions were monitored using previously optimized MRM settings programmed into a polarity switching

method (cytokinins and auxins detected in positive ion mode, others detected in negative ion mode). Analyst 1.6.2 software (SCIEX, Framingham, MA) was used for data acquisition; MultiQuant 3.0.2 software (SCIEX, Framingham, MA) was used for data analysis. The detected phytohormones were quantified based upon comparison of the analyte-to-internal standard integrated area ratios with a standard curve constructed using those same analytes, internal standards and internal standard concentrations (2.5 μM $^{13}C_6{}^{15}N$-JA-Ile; 0.10 μM d_5-*t*Z and d_5-*t*ZR; others 0.25 μM). The mixed calibration solutions were prepared over the range from 1.0 fmol to 100 pmol loaded on the column. The actual calibration range for each analyte was determined according to the concentrations of the analyte in samples.

ANE zoospore motility assay

Aliquots of *P. capsici* zoospore suspension at 10^6 zoospores/mL were distributed to a polystyrene ninety-six well plate (Fisher Scientific, Hampton, NH) and exposed to ANE such that the final concentrations per well were 0.1%, 0.2%, 0.3%, and 0.4% ANE. Sterile deionized water was used as a negative control. At 5, 10, and 15 minutes of exposure to their respective treatments, a hemocytometer was used to quantify vibrating and encysted zoospores per field of view. An overall motility status was also observed where fields of view with no motile zoospores remaining were reported. Using the standardized starting concentration, the overall motility status of the replicate, and the sum of encysted and vibrating zoospores and the number of lysed zoospores was calculated. Pathogen cultures were maintained and zoospore suspensions prepared as previously described (Dye, 2020)

Acknowledgements

Research supported in part by a Gates Millenium Scholars Program fellowship and Jastro-Shields awards to DCL, United States Department of Agriculture National Institute of Food and Agriculture grant 2021-67034-35049 to DMS, an NIH grant R35GM136402 to GC, and an unrestricted gift from Acadian Seaplants LTD to RMB. Sequencing was performed by the DNA Technologies and Expression Analysis Core at the UC Davis Genome Center, supported by NIH Shared Instrumentation Grant 1S10OD010786-01. Phytohormone analyses were performed by the Donald Danforth Plant Science Center, St. Louis, MO USA, based upon work supported by the National Science Foundation under Grant No. DBI-1427621 for acquisition of the QTRAP LC-MS/MS.

Author Contributions

Study planned by all authors. Experiments performed by DCL and analyzed by DCL, DMS, and RMB. Paper written by DCL and RMB, with editing by DMS and GLC.

Literature cited

Ali, N, Ramkissoon, A, Ramsubhag, A, and Jayaraj, J. (2016). *Ascophyllum* extract application causes reduction of disease levels in field tomatoes grown in a tropical environment. Crop Protect. 83, 67-75.

Andreou, A Z, Hornung, E, Kunze, S, Rosahl, S, and Feussner, I. (2009). On the substrate binding of linoleate 9-lipoxygenases. Lipids 44, 207-215.

Araceli, A-C, Elda, C-M, Edmundo, L-G, and Ernesto, G-P. (2007). Capsidiol production in pepper fruits (*Capsicum annuum L.*) induced by arachidonic acid is dependent of an oxidative burst. Physiol. Mol. Plant Pathol. 70, 69-76.

Bjornson, M, Pimprikar, P, Nürnberger, T, and Zipfel, C. (2021). The transcriptional landscape of *Arabidopsis thaliana* pattern-triggered immunity. Nat. Plants 7, 579-586.

Blankenberg, D, Von Kuster, G, Bouvier, E, Baker, D, Afgan, E, Stoler, N, Taylor, J, Nekrutenko, A, and Galaxy, T. (2014). Dissemination of scientific software with Galaxy ToolShed. Genome Biol. 15, 403.

Bostock, R M, Kuc, J A, and Laine, R A. (1981). Eicosapentaenoic and arachidonic acids from *Phytophthora infestans* elicit fungitoxic sesquiterpenes in the potato. Science 212, 67-69.

Chen, H, Chen, J, Li, M, Chang, M, Xu, K, Shang, Z, Zhao, Y, Palmer, I, Zhang, Y, McGill, J, Alfano, J R, Nishimura, M T, Liu, F, and Fu, Z Q. (2017). A bacterial type III effector targets the master regulator of salicylic acid signaling, NPR1, to subvert plant immunity. Cell Host Microbe 22, 777-788.e777.

Chini, A, Ben-Romdhane, W, Hassairi, A, and Aboul-Soud, M A M. (2017). Identification of TIFY/JAZ family genes in *Solanum lycopersicum* and their regulation in response to abiotic stresses. PLOS ONE 12, e0177381.

Choi, D, Ward, B L, and Bostock, R M. (1992). Differential induction and suppression of potato 3-hydroxy-3-methylglutaryl coenzyme A reductase genes in response to *Phytophthora infestans* and to its elicitor arachidonic acid. Plant Cell 4, 1333-1344.

Cook, J, Zhang, J, Norrie, J, Blal, B, and Cheng, Z. (2018). Seaweed extract (Stella Maris(®)) activates innate immune responses in *Arabidopsis thaliana* and protects host against bacterial pathogens. Mar. Drugs 16.

Creamer, J R, and Bostock, R M. (1986). Characterization and biological activity of *Phytophthora infestans* phospholipids in the hypersensitive response of potato tuber. Physiol. Mol. Plant Pathol. 28, 215-225.

Dave, A, and Graham, I A. (2012). Oxylipin signaling: a distinct role for the jasmonic acid precursor cis-(+)-12-oxo-phytodienoic acid (cis-OPDA). Front. Plant Sci. 3, 42-42.

Dileo, M V, Pye, M F, Roubtsova, T V, Duniway, J M, Macdonald, J D, Rizzo, D M, and Bostock, R M. (2010). Abscisic acid in salt stress predisposition to Phytophthora root and crown rot in tomato and chrysanthemum. Phytopathology 100, 871-879.

Du, M, Zhai, Q, Deng, L, Li, S, Li, H, Yan, L, Huang, Z, Wang, B, Jiang, H, Huang, T, Li, C-B, Wei, J, Kang, L, Li, J, and Li, C. (2014). Closely related NAC transcription factors of tomato differentially regulate stomatal closure and reopening during pathogen attack. Plant Cell 26, 3167-3184.

Dye, S M. (2020). Eicosapolyenoic fatty acids alter oxylipin gene expression and fatty acid hydroperoxide profiles in tomato and pepper roots. Physiol. Mol. Plant Pathol. v. 109, 2020 v.2109.

Dye, S M, and Bostock, R M. (2021). Eicosapolyenoic fatty acids induce defense responses and resistance to *Phytophthora capsici* in tomato and pepper. Physiol. Mol. Plant Pathol. 114, 101642.

Ewels, P, Magnusson, M, Lundin, S, and Käller, M. (2016). MultiQC: summarize analysis results for multiple tools and samples in a single report. Bioinformatics 32, 3047-3048.

Fidantsef, A, and Bostock, R. (1998). Characterization of potato tuber lipoxygenase cDNAs and lipoxygenase expression in potato tubers and leaves. Physiol. Plant. 102, 257-271.

Fournier, J, Pouénat, M-L, Rickauer, M, Rabinovltch-Chable, H, Rigaud, M, and Esquerré-Tugayé, M-T. (1993). Purification and characterization of elicitor-induced lipoxygenase in tobacco cells. Plant J. 3, 63-70.

Gellerman, J L, Anderson, W H, Richardson, D G, and Schlenk, H. (1975). Distribution of arachidonic and eicosapentaenoic acids in the lipids of mosses. Biochim. Biophys. Acta 388, 277-290.

Göbel, C, Feussner, I, Hamberg, M, and Rosahl, S. (2002). Oxylipin profiling in pathogen-infected potato leaves. Biochim. Biophys. Acta 1584, 55-64.

Göbel, C, Feussner, I, Schmidt, A, Scheel, D, Sanchez-Serrano, J, Hamberg, M, and Rosahl, S. (2001). Oxylipin profiling reveals the preferential stimulation of the 9-lipoxygenase pathway in elicitor-treated potato cells. J. Biol. Chem. 276, 6267-6273.

Goecks, J, Nekrutenko, A, Taylor, J, and The Galaxy, T. (2010). Galaxy: a comprehensive approach for supporting accessible, reproducible, and transparent computational research in the life sciences. Genome Biol. 11, R86.

Gómez-Gómez, L, Felix, G, and Boller, T. (1999). A single locus determines sensitivity to bacterial flagellin in *Arabidopsis thaliana*. Plant J. 18, 277-284.

Goñi, O, Fort, A, Quille, P, McKeown, P C, Spillane, C, and O'Connell, S. (2016). Comparative transcriptome analysis of two *Ascophyllum nodosum* extract biostimulants: same seaweed but different. J. Agric. Food Chem. 64, 2980-2989.

Hwang, I S, and Hwang, B K. (2010). The pepper 9-lipoxygenase gene CaLOX1 functions in defense and cell death responses to microbial pathogens. Plant Physiol. 152, 948-967.

Ishiga, Y, Ishiga, T, Uppalapati, S R, and Mysore, K S. (2013). Jasmonate ZIM-Domain (JAZ) protein regulates host and nonhost pathogen-induced cell death in tomato and *Nicotiana benthamiana*. PLOS ONE 8, e75728.

Jayaraj, J, Wan, A, Rahman, M, and Punja, Z K. (2008). Seaweed extract reduces foliar fungal diseases on carrot. Crop Protect. 27, 1360-1366.

Jogawat, A, Yadav, B, Chhaya, and Narayan, O P. (2021). Metal transporters in organelles and their roles in heavy metal transportation and sequestration mechanisms in plants. Physiol. Plant. 173, 259-275.

Klarzynski, O, Descamps, V, Plesse, B, Yvin, J-C, Kloareg, B, and Fritig, B. (2003). Sulfated fucan oligosaccharides elicit defense responses in tobacco and local and systemic resistance against Tobacco Mosaic Virus. Mol. Plant-Microbe Interact. 16, 115-122.

Knight, V I, Wang, H, Lincoln, J E, Lulai, E C, Gilchrist, D G, and Bostock, R M. (2001). Hydroperoxides of fatty acids induce programmed cell death in tomato protoplasts. Physiol. Mol. Plant Pathol. 59, 277-286.

Lal, N K, Nagalakshmi, U, Hurlburt, N K, Flores, R, Bak, A, Sone, P, Ma, X, Song, G, Walley, J, Shan, L, He, P, Casteel, C, Fisher, A J, and Dinesh-Kumar, S P. (2018). The receptor-like cytoplasmic kinase BIK1 localizes to the nucleus and regulates defense hormone expression during plant innate immunity. Cell Host Microbe 23, 485-497.e485.

Liao, Y, Smyth, G K, and Shi, W. (2013). featureCounts: an efficient general purpose program for assigning sequence reads to genomic features. Bioinformatics 30, 923-930.

Liu, J, Elmore, J M, Fuglsang, A T, Palmgren, M G, Staskawicz, B J, and Coaker, G. (2009). RIN4 functions with plasma membrane H^+-ATPases to regulate stomatal apertures during pathogen attack. PLoS Biol. 7, e1000139.

Lohman, B K, Weber, J N, and Bolnick, D I J M e r. (2016). Evaluation of TagSeq, a reliable low-cost alternative for RNA seq. Mol. Ecol. Resour. 16, 1315-1321.

Lorenzo, J M, Agregán, R, Munekata, P E S, Franco, D, Carballo, J, Şahin, S, Lacomba, R, and Barba, F J. (2017). Proximate composition and nutritional value of three macroalgae: *Ascophyllum nodosum*, *Fucus vesiculosus* and *Bifurcaria bifurcata*. Mar. Drugs 15, 360.

Love, M I, Huber, W, and Anders, S. (2014). Moderated estimation of fold change and dispersion for RNA-seq data with DESeq2. Genome Biol. 15, 550.

Meyer, E, Aglyamova, G, and Matz, M J M e. (2011). Profiling gene expression responses of coral larvae (*Acropora millepora*) to elevated temperature and settlement inducers using a novel RNA-Seq procedure. Mol. Ecol. 20, 3599-3616.

Mishina, T E, and Zeier, J. (2007). Pathogen-associated molecular pattern recognition rather than development of tissue necrosis contributes to bacterial induction of systemic acquired resistance in *Arabidopsis*. Plant J. 50, 500-513.

Ngou, B P M, Ding, P, and Jones, J D G. (2022). Thirty years of resistance: Zig-zag through the plant immune system. Plant Cell 34, 1447-1478.

Preisig, C L, and Kuć, J A. (1988). Metabolism by potato tuber of arachidonic acid, an elicitor of hypersensitive resistance. Physiol. Mol. Plant Pathol. 32, 77-88.

Ricker, K E, and Bostock, R M. (1992). Evidence for release of the elicitor arachidonic acid and its metabolites from sporangia of *Phytophthora infestans* during infection of potato. Physiol. Mol. Plant Pathol. 41, 61-72.

Ricker, K E, and Bostock, R M. (1994). Eicosanoids in the *Phytophthora infestans*-potato interaction: lipoxygenase metabolism of arachidonic acid and biological activities of selected lipoxygenase products. Physiol. Mol. Plant Pathol. 44, 65-80.

Robinson, S M, and Bostock, R M. (2015). β-glucans and eicosapolyenoic acids as MAMPs in plant-oomycete interactions: past and present. Front. Plant Sci. 5, 797-797.

Sangha, J S, Ravichandran, S, Prithiviraj, K, Critchley, A T, and Prithiviraj, B. (2010). Sulfated macroalgal polysaccharides λ-carrageenan and ι-carrageenan differentially alter *Arabidopsis thaliana* resistance to *Sclerotinia sclerotiorum* Physiol. Mol. Plant Pathol. 75, 38-45.

Savchenko, T, Walley, J W, Chehab, E W, Xiao, Y, Kaspi, R, Pye, M F, Mohamed, M E, Lazarus, C M, Bostock, R M, and Dehesh, K. (2010). Arachidonic acid: an evolutionarily conserved signaling molecule modulates plant stress signaling networks. Plant Cell 22, 3193-3205.

Shukla, P S, Mantin, E G, Adil, M, Bajpai, S, Critchley, A T, and Prithiviraj, B. (2019). *Ascophyllum nodosum*-based biostimulants: sustainable applications in agriculture for the stimulation of plant growth, stress tolerance, and disease management. Front. Plant Sci. 10.

Stermer, B A, and Bostock, R M. (1987). Involvement of 3-hydroxy-3-methylglutaryl coenzyme a reductase in the regulation of sesquiterpenoid phytoalexin synthesis in potato. Plant Physiol. 84, 404-408.

Subramanian, S, Sangha, J S, Gray, B A, Singh, R P, Hiltz, D, Critchley, A T, and Prithiviraj, B. (2011). Extracts of the marine brown macroalga, *Ascophyllum nodosum*, induce jasmonic acid dependent systemic resistance in *Arabidopsis thaliana* against *Pseudomonas syringae pv. tomato* DC3000 and *Sclerotinia sclerotiorum*. Eur. J. Plant Pathol. 131, 237-248.

Sun, X-C, Gao, Y-F, Li, H-R, Yang, S-Z, and Liu, Y-S. (2015). Over-expression of SlWRKY39 leads to enhanced resistance to multiple stress factors in tomato. J. Plant Biol. 58, 52-60.

Tsuda, K, Sato, M, Stoddard, T, Glazebrook, J, and Katagiri, F. (2009). Network properties of robust immunity in plants. PLoS Genet. 5, e1000772.

van Ginneken, V J, Helsper, J P, de Visser, W, van Keulen, H, and Brandenburg, W A. (2011). Polyunsaturated fatty acids in various macroalgal species from North Atlantic and tropical seas. Lipids Health Dis 10, 104.

Vera, J, Castro, J, Gonzalez, A, and Moenne, A. (2011). Seaweed polysaccharides and derived oligosaccharides stimulate defense responses and protection against pathogens in plants. Mar. Drugs 9, 2514-2525.

Véronési, C, Rickauer, M, Fournier, J, Pouénat, M L, and Esquerré-Tugayé, M T. (1996). Lipoxygenase gene expression in the tobacco-*Phytophthora parasitica nicotianae* interaction. Plant Physiol. 112, 997-1004.

Wan, W-L, Zhang, L, Pruitt, R, Zaidem, M, Brugman, R, Ma, X, Krol, E, Perraki, A, Kilian, J, Grossmann, G, Stahl, M, Shan, L, Zipfel, C, van Kan, J A L, Hedrich, R, Weigel, D, Gust, A A, and Nürnberger, T. (2019). Comparing *Arabidopsis* receptor kinase and receptor protein-mediated immune signaling reveals BIK1-dependent differences New Phytol. 221, 2080-2095.

Wang, W, and Wang, Z-Y. (2014). At the intersection of plant growth and immunity. Cell Host Microbe 15, 400-402.

Weber, H, Chételat, A, Caldelari, D, and Farmer, E E. (1999). Divinyl ether fatty acid synthesis in late blight-diseased potato leaves. Plant Cell 11, 485-494.

Young, M D, Wakefield, M J, Smyth, G K, and Oshlack, A. (2010). Gene ontology analysis for RNA-seq: accounting for selection bias. Genome Biol. 11, R14.

Zhang, H, Hu, Z, Lei, C, Zheng, C, Wang, J, Shao, S, Li, X, Xia, X, Cai, X, Zhou, J, Zhou, Y, Yu, J, Foyer, C H, and Shi, K. (2018). A plant phytosulfokine peptide initiates auxin-dependent immunity through cytosolic ca2+ signaling in tomato The Plant Cell 30, 652-667.

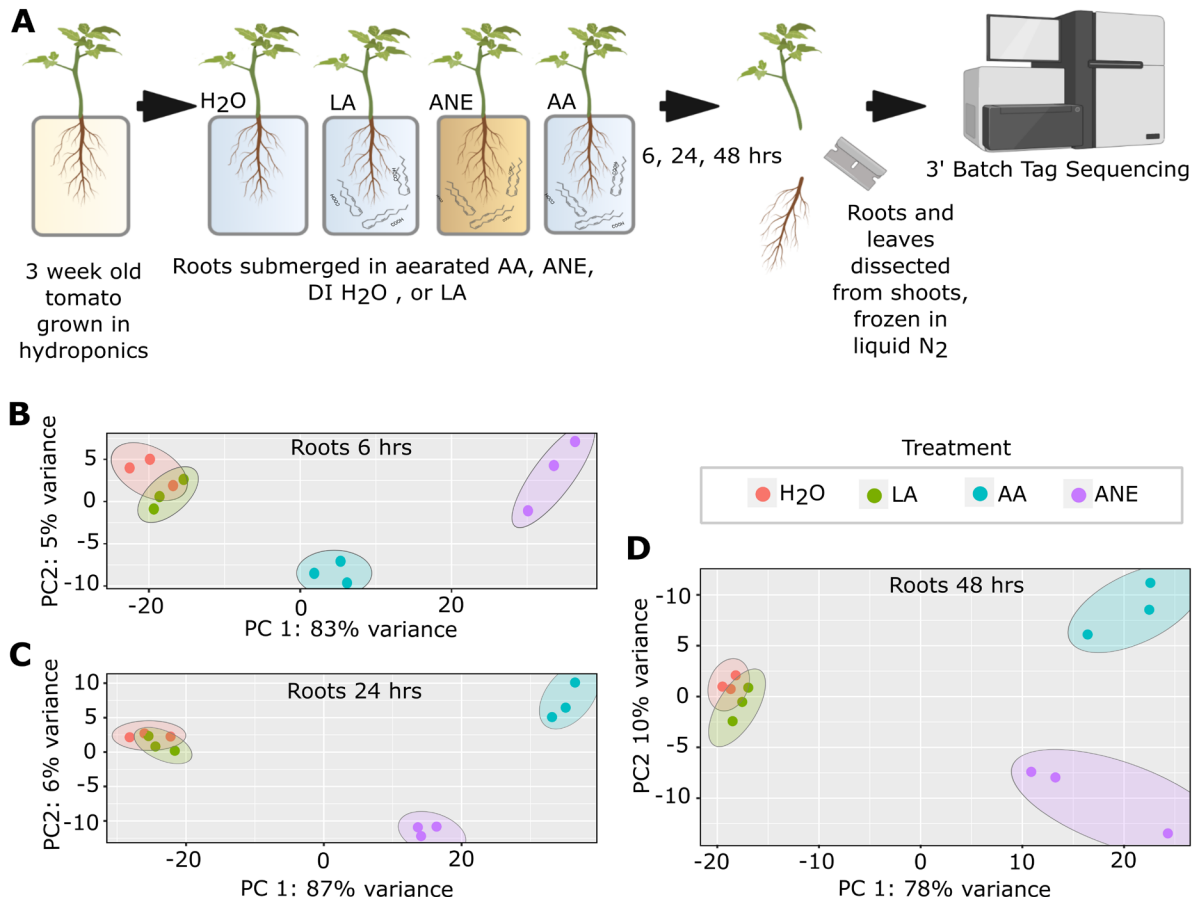

Figure 1. (A) Experimental procedure for RNA sequencing. Tomato roots treated with 10 µM Arachidonic Acid (AA), 0.4% Acadian (ANE), H_2O, or 10 µM Linoleic acid (LA). Following 6, 24, and 48 hours root exposure to their respective treatments, plants were harvested, root and leaf tissue dissected from shoots, and the collected tissue flash frozen in liquid nitrogen. Harvested tissue was then subjected to total RNA extraction and DNase treatment. All samples were submitted for quality control, RNA-seq library construction and 3'-Batch-Tag-Sequencing. Principle component analysis scatterplots of RNA sequencing data in roots after **(B)** 6, **(C)** 24, and **(D)** 48 hours of treatment with 10 µM AA, 0.4% ANE, H_2O, or 10 µM LA. PCA was conducted using the normalized read counts for all samples. PCA plots show variance of three biological replicates performed per timepoint and treatment.

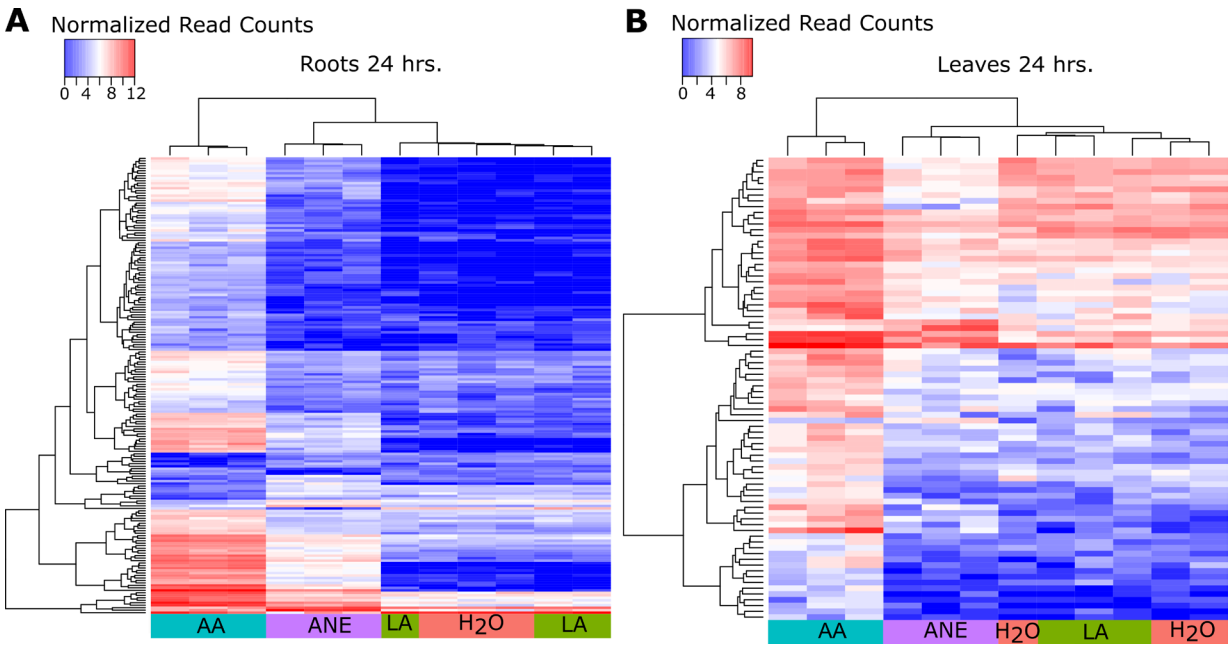

Figure 2. Normalized counts for the most differentially expressed genes by fold change for all treatment groups at 24 hours in **(A)** root and **(B)** leaf tissue. Plant roots were treated 10 µM Arachidonic Acid (AA), 0.4% Acadian (ANE), H_2O, or 10 µM Linoleic acid (LA) for 24 hours. Blue indicates significant gene suppression and red indicated significant gene induction for each treatment. Heatmap data is $\log_2$-transformed and hierarchically clustered. Differentially expressed genes require an adjusted *P*-value < 0.05 and an absolute fold change in gene expression >4 for roots and >2 for leaves.

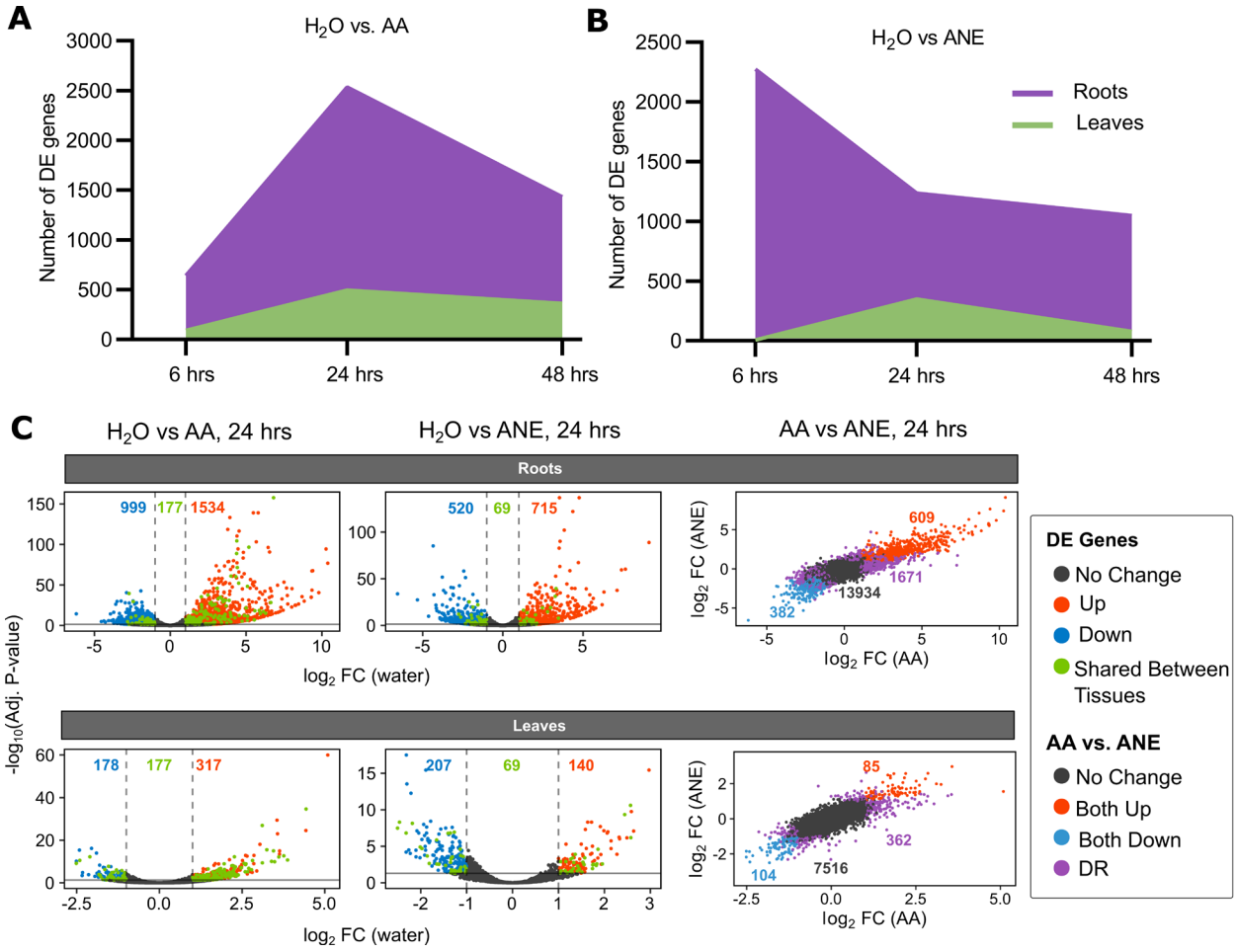

Figure 3. Total number of significant differentially expressed (DE) genes compared to H_2O by tissue across time points for **(A)** Arachidonic Acid (AA) and **(B)** Acadian (ANE) root-treated tomato. Plant roots were treated with H_2O, 10 µM LA, 10 µM AA, or 0.4% ANE for 6, 24 or 48 hours. **(C) Left:** Scatter plot of DE genes with the number of significantly up (red) and down (blue) regulated genes plotted at 24 hours from roots and leaves treated with AA or ANE compared to H_2O. Those DE genes shared between tissues within a treatment are colored green. Solid and dashed lines represent cutoffs for significant DE genes (adjusted *P*-value < 0.05 and an absolute fold change in gene expression >2). **Right:** Scatter plot of gene expression in response to AA vs. ANE within the same tissue colored by differential response: both no change (grey),

up regulated (red), and down regulated (blue) using the same significant cutoffs. Genes with different response between treatments are labeled DR (purple).

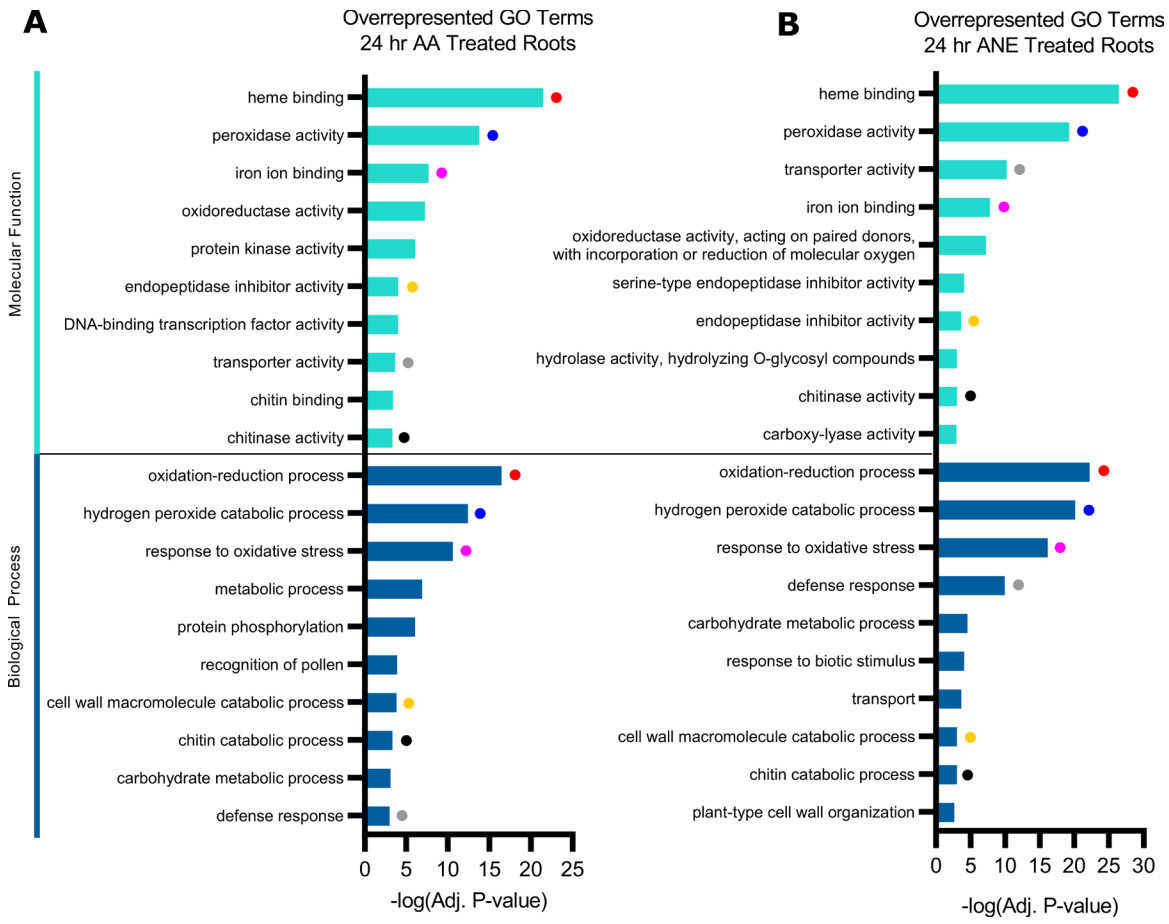

Figure 4. Gene ontology (GO) functional analysis of DE genes in roots 24 hours post-treatment. GO enrichment was conducted using Goseq. The top 10 most significantly (*P*-value < 0.05) enriched GO terms in molecular function and biological process GO categories are shown. Colored dots indicate shared molecular function and biological processes between **(A)** Arachidonic Acid (AA) and **(B)** Acadian (ANE) treatments. All adjusted *P*-values are negative 10-base log-transformed.

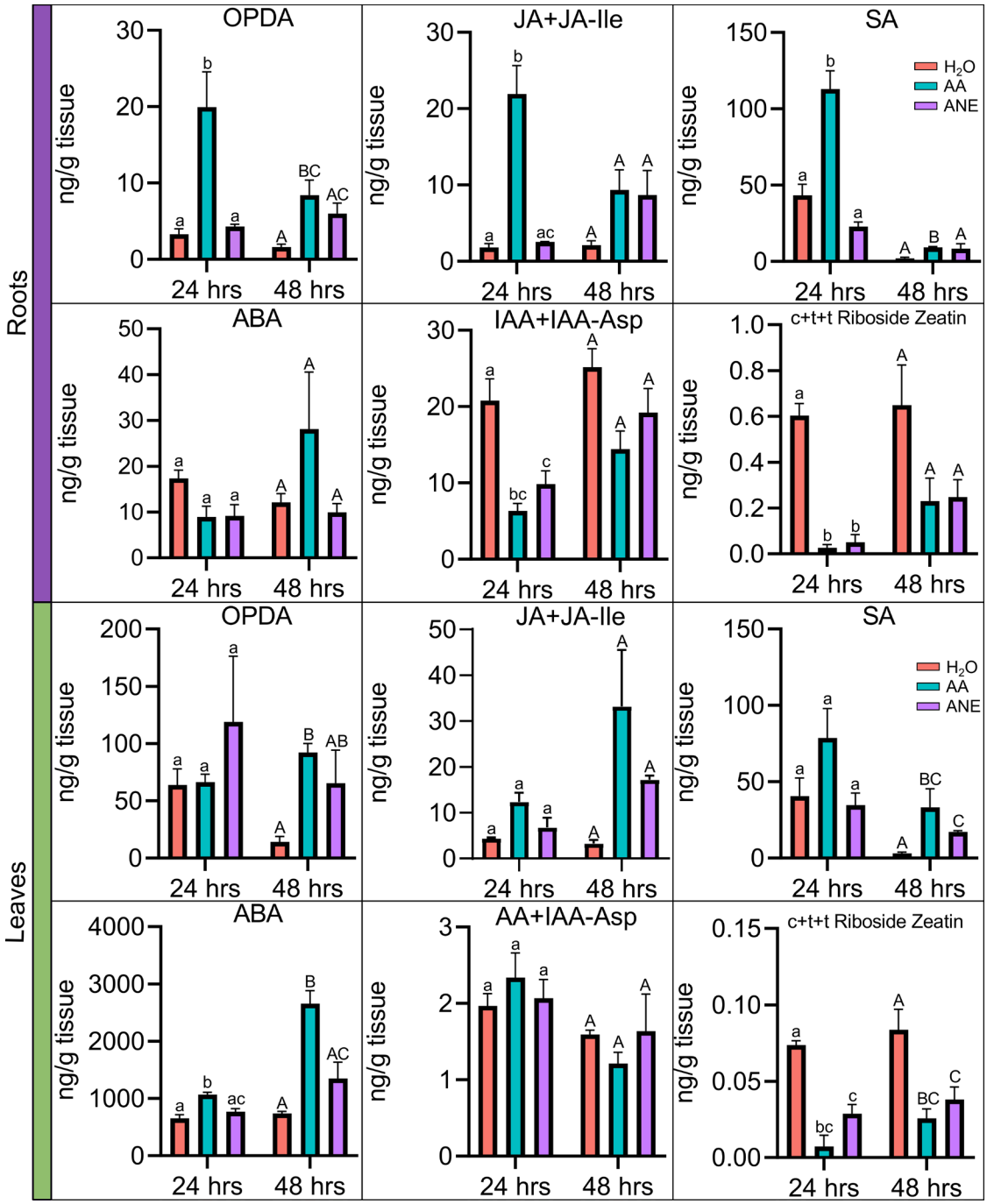

Figure 5. Quantification of phytohormones oxophytodienoic acid (OPDA), Jasmonic acid and JA-isoleucine (JA+JA-Ile), salicylic acid (SA), abscisic acid (ABA), indole acetic acid and IAA-aspartate (IAA+IAA-Asp), cis/trans zeatin and trans Riboside zeatin in **(A)** roots and **(B)** leaves of tomato seedlings root-treated with H_2O, 10 µM AA , or 0.4% ANE, for 24 and 48 hours.

Error bars represent standard error of 3 biological replicates. For bars with different letters, the difference of means is statistically significant by ANOVA and Tukey's HSD $P<0.05$. Lower-case letters denote statistical significance for 24 hours and upper-case letters denote statistical significance for 48 hours. All statistical comparisons are within a single timepoint and tissue type.

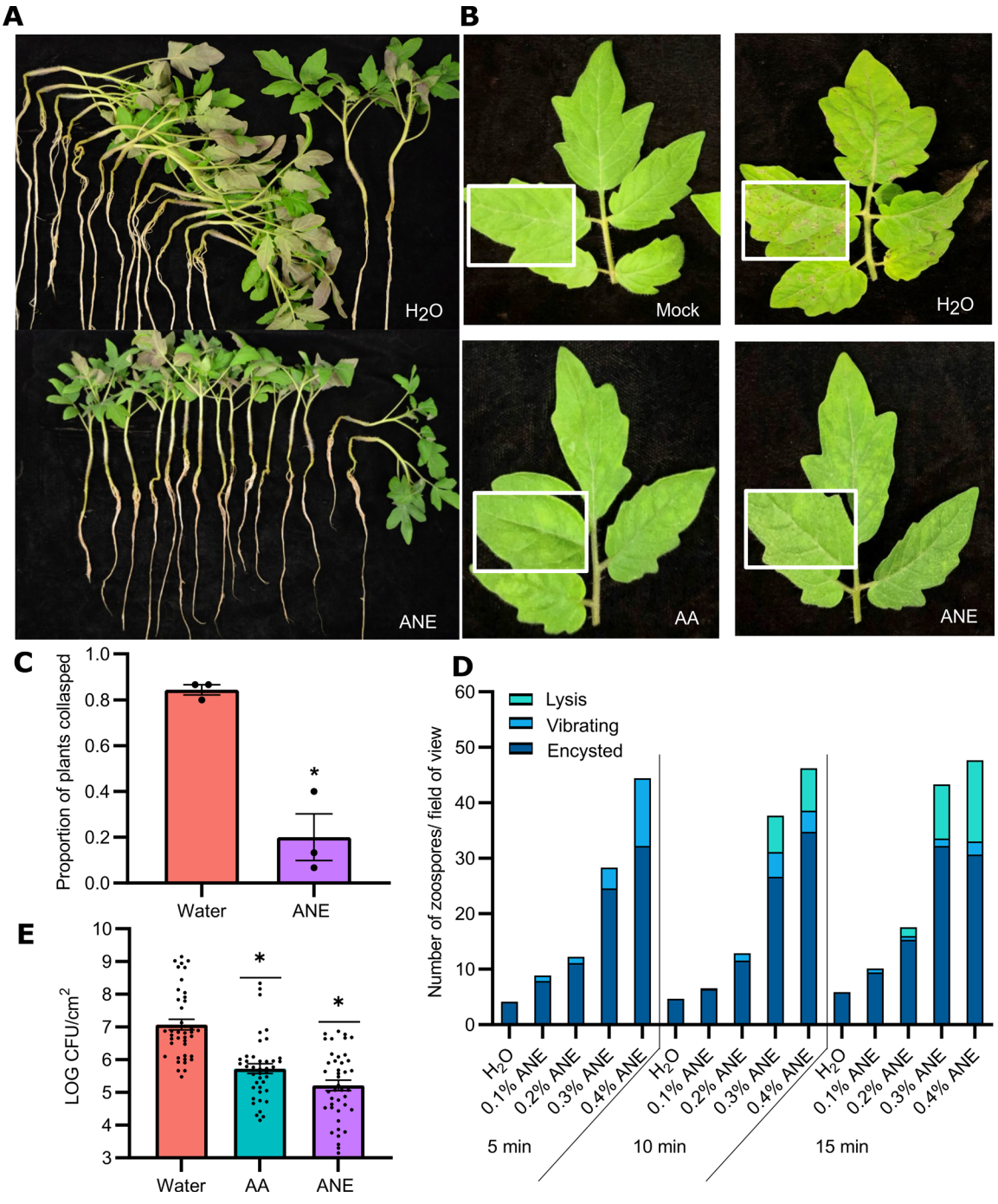

Figure 6. **(A)** Hydroponically grown tomato seedlings treated with 0.4% Acadian (ANE) or water 48 hours post inoculation with *Phytophthora capsici* zoospore suspension and rated on the incidence of collapse at the crown. **(C)** Data are the means and SE for 3 independent trials at 0.4% ANE with 15 plants per treatment per trial. * Significantly different by Wilcoxon rank

sums test, $X^2 = 3.97$, P< 0.046. **(B)** Representative leaf symptoms on hydroponically grown tomato root treated with 0.4% ANE, 10uM Arachidonic Acid (AA), or water 72 hours post spray inoculation with *Pseudomonas syringae* pv. *tomato* bacterial suspension in 10 mM $MgCl_2$ at OD^{600}= 0.3. Bacterial colonization as measured by LOG colony forming units (CFU) per cm^2 of leaf tissue72 hours post-inoculation **(E)**. Data are the means and SE for 3 independent trials with n=14 per trial. * Significantly different by Tukey's HSD P<0.0001. **(D)** Direct effect of 0.1%, 0.2%, 0.3% and 0.4% ANE on zoospore motility at 5, 10, and 15 minutes of exposure. The number of lysed, vibrating, and encysted zoospores per field of view. Data are the means for 3 independent trials with n=3 per treatment concentration and timepoint per trial.

				AA 24 hr Roots		ANE 24 hr Roots	
Pathway	**Gene ID**	**Annotation**	**Gene Name**	**Log2FC**	**adj. p-value**	**Log2FC**	**adj. p-value**
LOX Pathway	Solyc02g087070.3	alpha-DOX1	NA	6.656877	3.952504e-43	4.735599	2.393123e-21
	Solyc01g109140.3	divinyl ether synthase (9-divinyl ether synthase)	DES	6.451561	5.252232e-97	4.057925	6.092980e-32
	Solyc08g029000.3	Lipoxygenase (AHRD V3.3 *** Q43800_TOBAC)	9-LOX	5.670189	6.059722e-104	3.991129	3.722707e-45
	Solyc10g007960.1	Allene oxide synthase (AHRD V3.3 *** Q5NDE2_SOLTU) (Allene oxide synthase 3)	AOS3	1.685647	3.360501e-04	2.371630	5.336512e-04
WRKY TFs	Solyc05g015850.3	WRKY transcription factor 75	SLWRKY75	7.074404	2.312198e-50	5.419730	1.650934e-33
	Solyc08g067340.3	WRKY transcription factor 46	SLWRKY46	4.277548	3.244409e-13	2.881808	2.501558e-05
	Solyc03g116890.3	WRKY transcription factor 39	SLWRKY39	3.642748	8.280043e-32	1.874182	8.433876e-07
	Solyc09g015770.3	WRKY transcription factor 81	WRKY3	3.306811	1.054946e-35	1.735481	6.997109e-06
MAPKs	Solyc02g090970.1	MAP kinase kinase kinase 21	NA	5.000521	3.058998e-10	2.458481	6.761017e-03
	Solyc02g071740.3	MAP kinase kinase kinase 16	NA	2.606496	1.181915e-25	1.029662	1.057492e-03
Receptors	Solyc07g008620.1	EIX receptor 1	EIX1	3.669240	3.272107e-08	2.214993	8.598968e-03
	Solyc06g071810.1	Leucine-rich repeat receptor-like kinase (AHRD V3.3 *** K4C8Q3_SOLLC)	SOBIR1	1.886638	4.219792e-08	1.218518	4.244156e-03
JA Signaling	Solyc07g063410.3	JA2-like	JA2L	3.992618	4.410113e-13	2.044361	9.816992e-03
	Solyc12g013620.2	jasmonic acid 2	JA2	5.092760	5.312364e-12	3.668141	2.790927e-07
	Solyc08g036660.3	Jasmonate zim-domain protein (AHRD V3.3 *** G7IP70_MEDTR)	SlJAZ11	6.727738	7.883234e-15	2.877514	1.674547e-03
	Solyc11g011030.2	Pto-responsive gene 1	JAZ7	3.293363	2.058116e-07	2.035988	9.624008e-03
SA Signaling	Solyc07g044980.3	NIM1-like protein 2	NML2/ NPR1	1.168013	5.142510e-07	1.082963	8.851628e-07
Ethylene Signaling	Solyc09g066360.1	Ethylene Response Factor C.3	ERF.C.3	8.251996	9.922638e-26	4.436850	2.455116e-09
	Solyc09g089610.3	ethylene receptor-like protein (ETR6)	ETR6	3.249116	4.072273e-03	2.494971	8.128305e-03
	Solyc06g053710.3	ethylene receptor homolog (ETR4)	ETR4	3.011504	2.959852e-21	2.267110	3.805192e-11
	Solyc09g075420.3	ethylene response factor E.1	ERF2	1.932686	1.137574e-02	2.708430	7.191094e-17
2° Metabolism	Solyc01g101170.3	Viridiflorene synthase (AHRD V3.3 *** TPS31_SOLLC)	TPS31	9.293983	2.134563e-35	5.660419	6.637793e-18
	Solyc04g072280.3	Laccase (AHRD V3.3 *** A0A022Q9N6_ERYGU)	NA	6.948967	3.476060e-16	3.697150	4.491432e-06
	Solyc02g038740.3	3-hydroxy-3-methylglutaryl coenzyme A reductase (AHRD V3.3 *** K4B5W7_SOLLC)	HMG2	6.546776	2.241348e-91	3.571600	2.001060e-21
	Solyc08g007790.3	3-hydroxy-3-methylglutaryl coenzyme A synthase	HMGS	4.819941	6.790517e-91	2.350877	4.449196e-16
	Solyc02g078650.3	Polyphenol oxidase (AHRD V3.3 *** A0A118JXA6_CYNCS)	NA	3.928785	5.125454e-134	2.310150	1.558317e-41
	Solyc08g068730.1	Tyramine n-hydroxycinnamoyl transferase (AHRD V3.3 *** Q5D8C0_CAPAN)	THT1-3	3.412020	4.833930e-29	2.571582	7.327733e-07
	Solyc10g011920.2	Phenylalanine ammonia-lyase (AHRD V3.3 *** A0A124SBF6_CYNCS)	PAL	3.735867	5.023393e-13	2.152346	1.365268e-03
	Solyc04g049350.3	chorismate synthase 1 precursor (chorismate synthase 1)	CS1	1.663705	2.269832e-17	1.021305	2.146662e-09
PR	Solyc06g061215.1	Proteinase inhibitor II (AHRD V3.3 *-* B3F0C1_TOBAC)	NA	10.271308	4.417542e-95	7.396038	2.945058e-60
	Solyc06g076170.3	Glucan endo-1,3-beta-glucosidase, putative (AHRD V3.3 *** B9T3M9_RICCO)	NA	7.747762	3.541570e-27	5.511062	5.238145e-19
	Solyc00g174330.3	Pathogenesis related protein PR-1//Pathogenesis-related leaf protein 4	PR1 (P6)	6.520672	5.184005e-16	5.402830	5.765970e-22
	Solyc02g082920.3	acidic extracellular 26 kD chitinase	CHI3	5.870717	2.842767e-19	4.985453	3.760754e-20
	Solyc05g050870.3	Peroxidase (AHRD V3.3 *** K4C1C0_SOLLC)	NA	4.745316	1.246767e-10	4.424698	3.852836e-13
	Solyc01g087820.2	subtilisin-like protease 4B	sbt4B	1.571173	3.557181e-07	1.748230	4.607271e-12

Figure 7. Significantly up-regulated genes shared by Arachidonic Acid (AA) and Acadian (ANE) treated roots at 24 hours. Log_2-fold change and adjusted *P*-values shown of all genes.

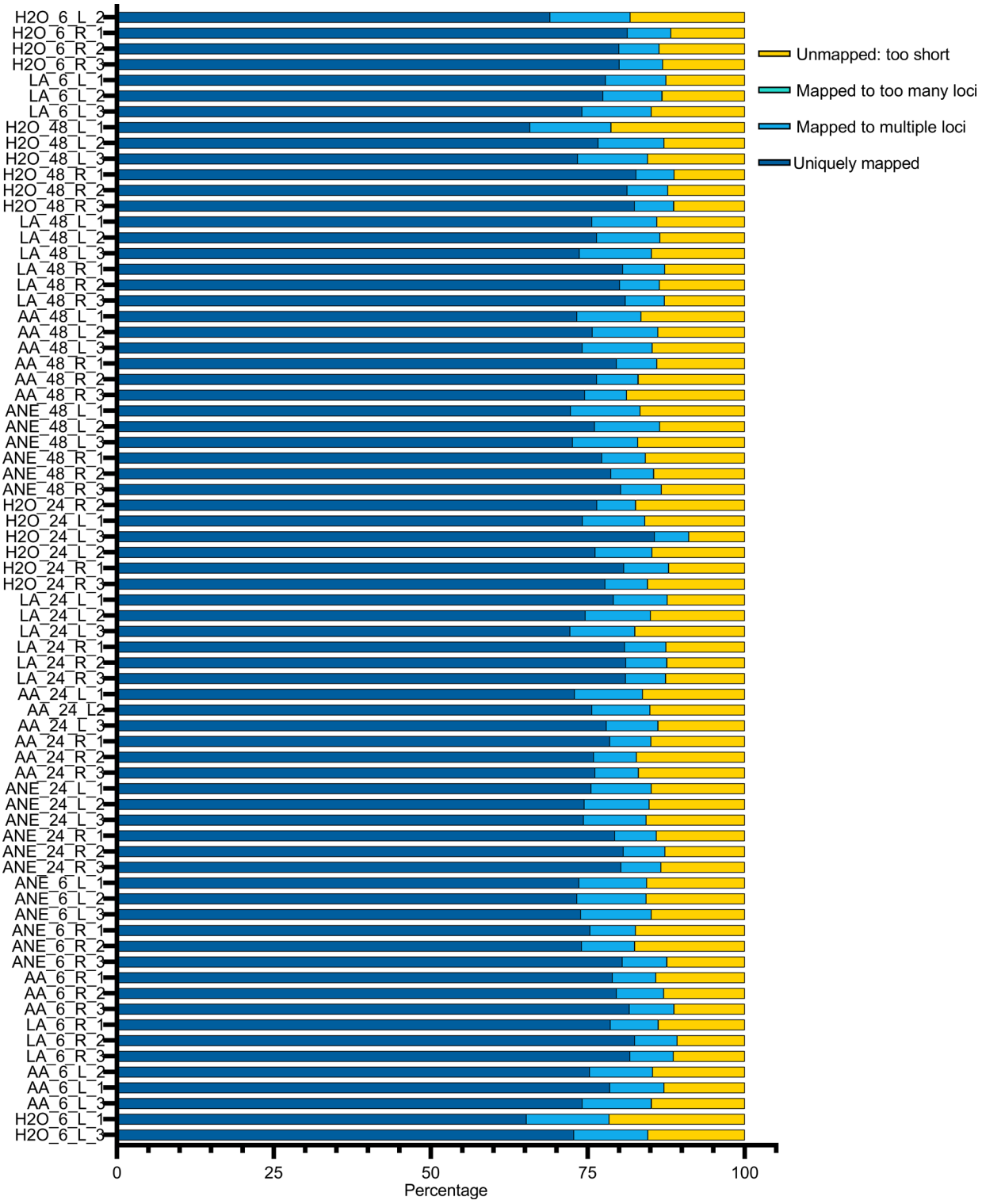

Supplementary Figure 1. Percent of sequencing reads that uniquely mapped, mapped to multiple loci, mapped to many loci, and too short unmapped reads to the tomato genome build SL 3.0. Tomato roots were treated with 10 µM Arachidonic Acid (AA), 0.4% Acadian (ANE),

H_2O, or 10 μM Linoleic acid (LA). Following 6, 24, and 48 hours root exposure to their respective treatments, plants were harvested, root (R) and leaf (L) samples were processed and subjected to RNA sequencing. Alignment was conducted using RNA STAR aligner accessed through the Galaxy toolshed.

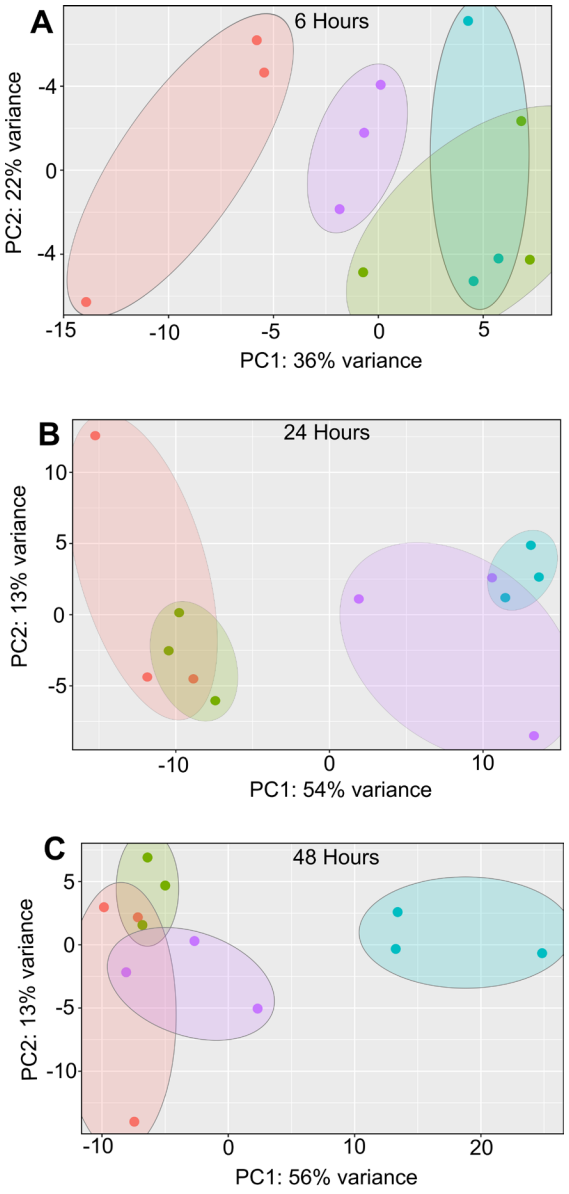

Supplemental Figure 2. Principle component analysis scatterplots of RNA sequencing data in leaves after **(A)** 6, **(B)** 24, and **(C)** 48 hours of treatment with 10 µM Arachidonic Acid (AA), 0.4% Acadian (ANE), H_2O, or 10 µM Linoleic acid (LA). PCA was conducted using the normalized read counts for all samples. PCA plots show variance of three biological replicates performed per timepoint and treatment.

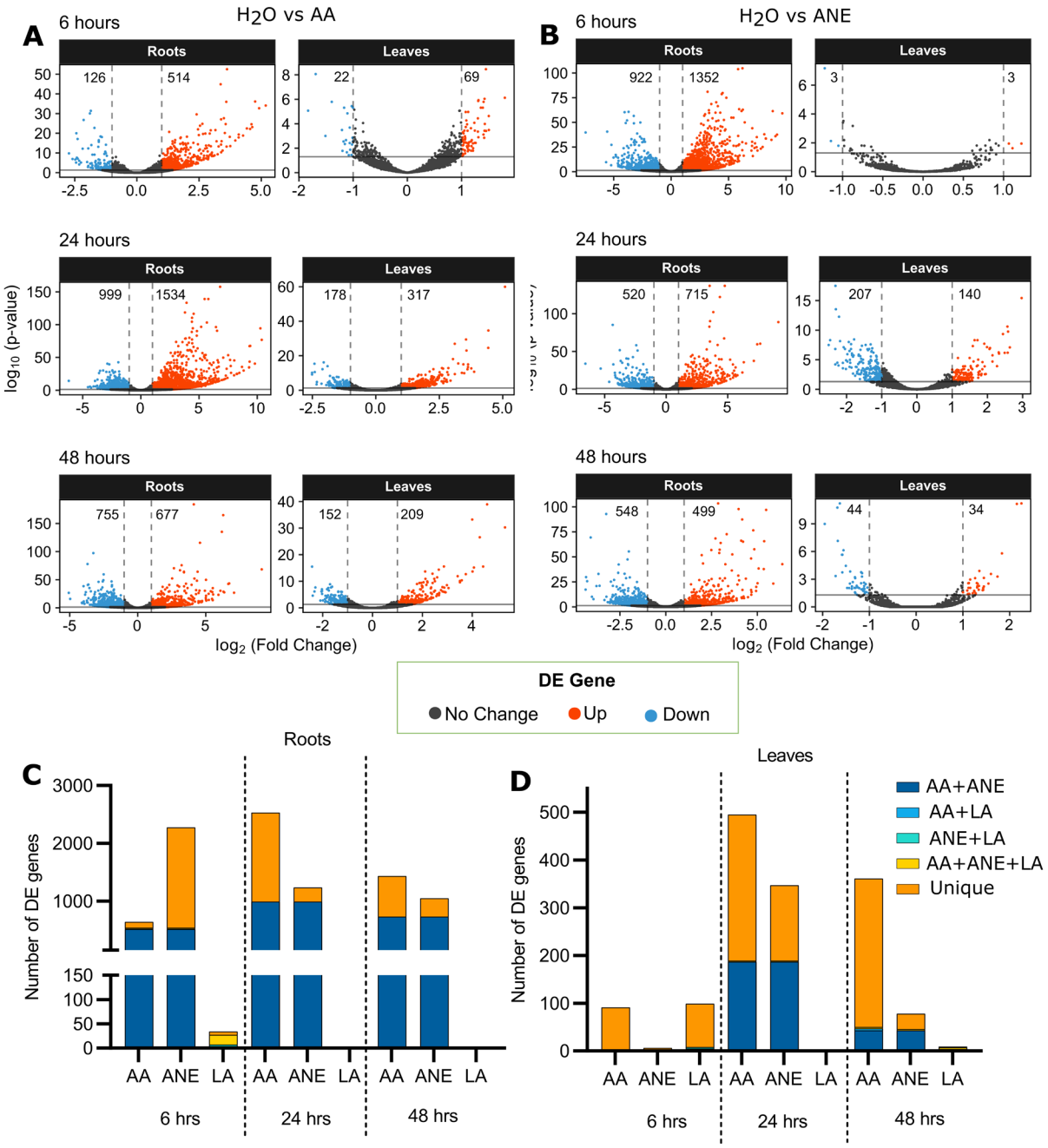

Supplemental Figure 3. Scatter plot of DE genes with the number of significantly up (red) and down (blue) regulated genes plotted from roots and leaves treated with AA **(A)** or ANE **(B)** compared to H_2O-treated tissue across time points. Solid and dashed lines represent cutoffs for significant DE genes (adjusted *P*-value < 0.05 and an absolute fold change in gene expression

>2). Number of DE genes shared and unique between AA, ANE, and Linoleic acid (LA) compared to H_2O in **(C)** roots and **(D)** leaves. Plant roots were treated with H_2O, 10 μM LA, 10 μM AA, or 0.4% ANE for 6, 24 or 48 hours. DE genes compared to H_2O have an adjusted *P*-value < 0.05 and an absolute fold change in gene expression >2.

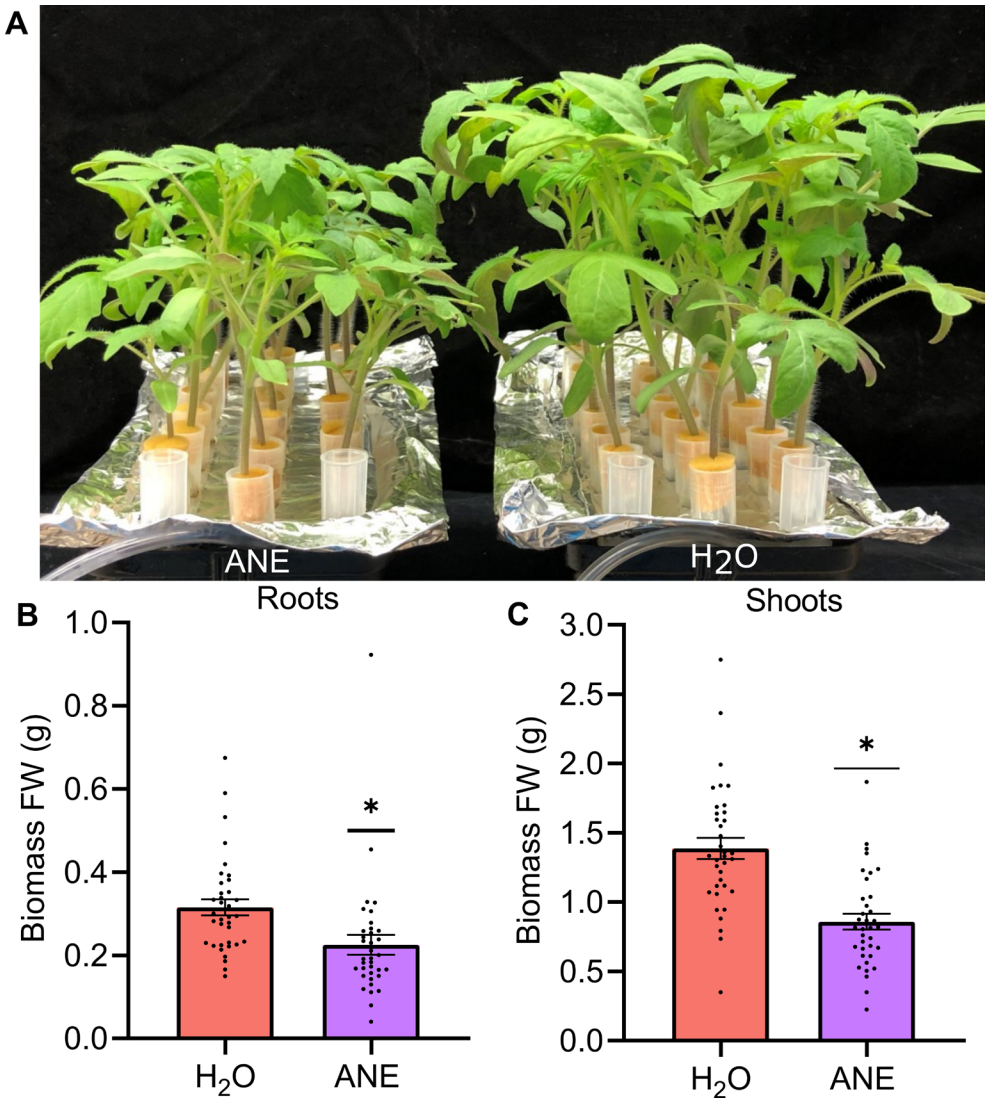

Supplemental Figure 4. (A) Acadian (ANE)-associated growth penalty in hydroponically-reared tomato 72 hours post treatment with 0.4% ANE. Treatment effect on fresh weight biomass of **(B)** roots and **(C)** shoots. Data are the means and SE for 2 independent trials at 0.4% ANE with 18 plants per treatment per trial. * Significantly different by Student's t test, $P<$ 0.0048 (Panel B) and $P<0.0001$ (Panel C). Error bars represent standard error of 2 biological replicates.

AAvsH2O Roots 24 Hrs. Under represented								
GO Category	Over_rep_Pval	Under_rep_Pval	NumDEInCat	NumInCat	Term Details	Ontology	PadjOver	PadjUnder
GO:0006281	0.999999989	2.41E-07	1	87	DNA repair	BP	1	4.71E-05
GO:0000166	0.99999999	2.84E-08	25	312	nucleotide binding	MF	1	6.19E-06
GO:0003723	1	1.81E-09	15	247	RNA binding	MF	1	4.43E-07
GO:0003676	1	0	27	542	nucleic acid binding	MF	1	0
GO:0003735	1	0	5	301	structural constituent	MF	1	0
GO:0005622	1	0	10	316	intracellular	CC	1	0
GO:0005840	1	0	5	289	ribosome	CC	1	0
GO:0006412	1	0	5	306	translation	BP	1	0
GO:0008270	1	0	68	701	zinc ion binding	MF	1	0
GO:0005515	1	0	303	2165	protein binding	MF	1	0

ANEvsH2O Roots 24 Hrs. Under represented								
GO Category	Over_rep_Pval	Under_rep_Pval	NumDEInCat	NumInCat	Term Details	Ontology	PadjOver	PadjUnder
GO:0000166	0.999966464	9.46E-05	12	306	nucleotide binding	MF	1	0.019931
GO:0005525	0.999974124	0.00010226	6	196	GTP binding	MF	1	0.019931
GO:0003723	0.999999909	5.27E-07	5	246	RNA binding	MF	1	0.000128
GO:0008270	1	1.06E-09	27	677	zinc ion binding	MF	1	2.95E-07
GO:0005622	1	1.81E-10	7	315	intracellular	CC	1	5.87E-08
GO:0003676	1	0	6	536	nucleic acid binding	MF	1	0
GO:0006412	1	0	3	302	translation	BP	1	0
GO:0005515	1	0	119	2117	protein binding	MF	1	0
GO:0003735	1	0	4	299	structural constituent	MF	1	0
GO:0005840	1	0	4	287	ribosome	CC	1	0

BP	Biological Process
MF	Molecular Function
CC	Cellular Compartment

Supplemental Table 1. Gene ontology functional analysis displaying underrepresented GO terms and associated adjusted P-values for Arachidonic Acid (AA) and Acadian (ANE) treated roots at 24 hours.

		AA 24 hr Roots		ANE 24 hr Roots	
Gene ID	ITAG 3.2 Annotation	log2FC	adj. p-value	log2FC	adj. p-value
Solyc02g069200.2	iron-regulated transporter 1	-6.196168495	5.00233E-15	-6.566816937	1.43E-34
Solyc03g093390.3	beta expansin precursor 2	-3.507406176	2.41236E-30	-2.439554434	2.24E-06
Solyc05g015350.3	Cytochrome P450 (AHRD V3.3 *** A0A103XVZ6_CYNCS)	-3.721646202	0.001532442	-2.183374715	0.024372283
Solyc06g007960.3	Caffeic O-methyltransferase (AHRD V3.3 *** A0A068FLE8_PUNGR)	-3.729352108	6.12561E-17	-3.028227931	1.96E-14
Solyc07g006855.1	CASP-like protein (AHRD V3.3 *** M1BM50_SOLTU)	-4.277908246	8.41046E-05	-2.271651304	0.006864866
Solyc07g008420.3	Blue copper (AHRD V3.3 *** A0A0B0N2W0_GOSAR)	-3.878110634	1.34202E-06	-3.198519365	2.24E-06
Solyc07g009310.3	LOW QUALITY:defensin-like protein (AHRD V3.3 -** AT1G19610.1)	-3.536243084	5.96685E-05	-3.260246094	6.33E-05
Solyc07g061840.1	LOW QUALITY:Bifunctional inhibitor/lipid-transfer protein/seed storage 2S albumin superfamily protein (AHRD V3.3 -** AT1G66850.1)	-3.490276268	0.00392208	-2.547051715	0.008111773
Solyc07g061850.1	LOW QUALITY:AT hook motif DNA-binding family protein (AHRD V3.3 --* AT1G63480.7)	-3.661297997	0.000474098	-3.240391122	0.000159208
Solyc08g005960.2	Bifunctional inhibitor/lipid-transfer protein/seed storage 2S albumin superfamily protein (AHRD V3.3 *** AT2G45180.1)	-3.594248127	7.27177E-27	-4.296944416	1.27E-33
Solyc08g007570.3	Homeobox-leucine zipper protein HOX9, putative (AHRD V3.3 *** A0A061DUZ5_THECC)	-4.373703204	3.28511E-06	-2.207637942	0.002163056
Solyc09g014870.1	Copper transporter family protein (AHRD V3.3 *** B9HPB1_POPTR)	-3.942919214	6.725E-15	-4.116896714	1.43E-16
Solyc11g018530.2	root-specific metal transporter	-4.063934849	1.33291E-06	-3.328204835	1.10E-05
Solyc12g042980.2	2-oxoglutarate-dependent dioxygenase (AHRD V3.3 *** A0A061G9S7_THECC)	-4.543858892	1.60808E-05	-3.565715043	2.07E-05
Solyc12g100300.2	Metal tolerance protein (AHRD V3.3 *** D7RJ71_CARPA)	-3.755764332	1.0061E-07	-4.630809886	1.42E-10

Supplemental Table 2. Top 15 shared genes most strongly downregulated in roots in response to Arachidonic Acid (AA) and Acadian (ANE) treatment at 24 hours.

AA Unique Up Top 15 by FC				
Gene ID	**log2FC**	**adj P-value**	**ITAG 3.2 Annotation**	**Gene Name**
Solyc01g095080.3	7.296116847	5.13E-23	1-aminocyclopropane-1-carboxylic acid synthase-2	ACS2
Solyc06g065060.2	7.247759814	4.28E-18	FAD-binding Berberine family protein (AHRD V3.3 *** A0A061GF79_THECC)	
Solyc04g072375.1	6.058685472	3.08E-11	LOW QUALITY:RING/U-box superfamily protein (AHRD V3.3 *-* AT1G63840.1)	
Solyc03g005040.1	6.008331931	7.35E-14	Calcium-binding protein (AHRD V3.3 *** A0A199V9T9_ANACO)	
Solyc03g098700.1	5.55822268	6.54E-09	Kunitz-type protease inhibitor D (AHRD V3.3 *** M1LA62_SOLTU)	
Solyc02g092120.3	5.512964465	9.50E-09	Phytosulfokines 3 family protein (AHRD V3.3 *** B9IBM1_POPTR)	PKS3L
Solyc10g005440.2	5.242053377	1.08E-07	Serine/threonine-protein kinase (AHRD V3.3 *** A0A0V0IWF8_SOLCH)	
Solyc11g044840.2	5.14264118	4.64E-11	Aspartate aminotransferase, putative (AHRD V3.3 *** B9T7N8_RICCO)	
Solyc03g113810.1	5.107425487	3.07E-07	LOW QUALITY:CDP-diacylglycerol--glycerol-3-phosphate 3-phosphatidyltransferase, putative (AHRD V3.3 *** A0A061FTS5_THECC)	
Solyc03g082520.1	5.036813691	4.75E-20	Small auxin up-regulated RNA36	SAUR36
Solyc08g021870.2	5.024214207	6.20E-07	Ankyrin repeat-containing protein (AHRD V3.3 *-* A0A124SAK7_CYNCS)	
Solyc07g052120.3	5.023539051	5.85E-07	Sesquiterpene synthase (AHRD V3.3 *-* G8H5N2_SOLHA)	
Solyc05g046340.2	4.999147528	7.10E-07	Phosphomannomutase (AHRD V3.3 *** K4C0W7_SOLLC)	
Solyc03g025640.2	4.987013198	1.62E-08	Cytochrome P450 (AHRD V3.3 *** I6YHZ8_LINUS)	
Solyc07g006930.1	4.940427969	1.25E-06	LOW QUALITY:transmembrane protein, putative (DUF247) (AHRD V3.3 *** AT3G02645.1)	
AA Unique Down Top 15 by FC				
Solyc11g045520.2	-3.724032716	1.45E-03	1-AMINOCYCLOPROPANE-1-CARBOXYLATE OXIDASE-like protein	ACO
Solyc10g011730.3	-3.675442677	3.63E-04	Arabinogalactan peptide 20 (AHRD V3.3 *** AGP20_ARATH)	AGP20
Solyc02g032030.1	-3.523525682	1.37E-06	Dirigent protein (AHRD V3.3 *** K4B5E9_SOLLC)	
Solyc05g009180.1	-3.359559112	3.74E-05	LOW QUALITY:Zinc finger family protein (AHRD V3.3 *** B9HWF8_POPTR)	
Solyc11g005610.1	-3.261823247	8.57E-03	LOW QUALITY:GRAS family transcription factor (AHRD V3.3 *** G7LD66_MEDTR)	
Solyc09g059170.2	-3.259677665	8.73E-03	Glycosyltransferase (AHRD V3.3 *** M1C989_SOLTU)	
Solyc06g075040.1	-3.245800186	3.17E-03	Auxin efflux carrier family protein (AHRD V3.3 --* AT1G23080.4)	
Solyc04g074340.3	-3.154792841	4.24E-06	Glycosyltransferase (AHRD V3.3 *** K4BTX1_SOLLC)	
Solyc09g008910.2	-3.096979401	1.35E-06	Cytochrome P450 (AHRD V3.3 *** A0A061ETV7_THECC)	
Solyc11g011000.2	-3.06812522	1.67E-02	Cysteine-rich repeat secretory protein 60 (AHRD V3.3 *** A0A061EEI8_THECC)	
Solyc09g082900.3	-3.052023255	2.61E-03	4-hydroxy-3-methylbut-2-enyl diphosphate synthase (AHRD V3.3 --* AT5G60600.5)	
Solyc07g042600.2	-3.038861181	1.89E-02	Transposon-like element Lyt2-2 DNA (AHRD V3.3 *** D5MNY6_SOLLC)	
Solyc12g007010.2	-3.038300161	1.84E-02	fe-S cluster assembly factor HCF101	
Solyc10g081690.1	-2.984073654	1.14E-02	LOW QUALITY:Transmembrane protein, putative (AHRD V3.3 *** A0A072UES2_MEDTR)	
Solyc01g095440.2	-2.971594786	2.24E-02	LOW QUALITY:transmembrane protein, putative (DUF1191) (AHRD V3.3 *** AT4G01140.1)	

ANE Unique Up Top 15 by FC				Gene Name
Gene ID	**log2FC**	**adj P-value**	**ITAG 3.2 Annotation**	
Solyc07g054790.1	4.706195351	1.93E-13	Wound-responsive family protein (AHRD V3.3 *** A0A061E3U8_THECC)	
Solyc05g053860.3	3.062117334	1.28E-06	Organic cation/carnitine transporter (AHRD V3.3 *** A0A072TPM4_MEDTR)	
Solyc09g097810.3	2.974612031	5.64E-05	SAR8.2 (AHRD V3.3 *** Q9SEM2_CAPAN)	SAR8.2
Solyc01g100980.3	2.945950383	5.81E-04	Pectin lyase-like superfamily protein (AHRD V3.3 *** AT1G02460.1)	
Solyc06g068270.3	2.79141393	9.26E-04	2-oxoglutarate (2OG) and Fe(II)-dependent oxygenase superfamily protein (AHRD V3.3 *** AT1G49390.1)	
Solyc01g088160.3	2.767232958	1.98E-03	cytokinin oxidase2	CKX2
Solyc07g054760.1	2.720747917	4.16E-08	LOW QUALITY:Wound-responsive family protein (AHRD V3.3 *** AT4G10265.1)	
Solyc05g008880.1	2.697670904	1.79E-03	LOW QUALITY:proline transporter 2 (AHRD V3.3 --* AT3G55740.3)	
Solyc04g014400.3	2.695395712	3.92E-06	LRR receptor-like kinase (AHRD V3.3 *-* A0A072U1S2_MEDTR)	
Solyc04g077990.3	2.692437255	4.23E-03	LOB domain-containing protein, putative (AHRD V3.3 *** B9SND0_RICCO)	
Solyc10g050990.1	2.368948298	1.79E-02	Pyruvate kinase (AHRD V3.3 --* A9TZX1_PHYPA)	
Solyc07g007250.3	2.351970636	1.74E-02	Metallocarboxypeptidase inhibitor (AHRD V3.3 *** MCPI_SOLLC)	TCMP-1
Solyc01g008640.3	2.328061039	1.53E-03	Cytochrome P450 (AHRD V3.3 *** Q9AVQ2_SOLTU)	
Solyc06g084070.3	2.306751041	1.02E-06	auxin-regulated IAA2	IAA2
Solyc06g008300.3	2.296015865	8.45E-03	Leucine-rich repeat receptor-like protein kinase family protein (AHRD V3.3 *** AT4G08850.1)	
ANE Unique Down Top 15 by FC				
Solyc05g006190.1	-3.913438144	6.08E-08	LOW QUALITY:O-acyltransferase (AHRD V3.3 --* T2HV99_EUPLA)	
Solyc04g051270.2	-3.183752109	4.81E-06	CASP-like protein (AHRD V3.3 *** K4BS87_SOLLC)	
Solyc09g015240.2	-3.099753397	3.84E-04	Uncharactized protein	
Solyc01g079270.1	-3.010633519	6.71E-04	Transcription factor, putative (AHRD V3.3 *-* B9RNB4_RICCO)	
Solyc02g082090.3	-3.00246873	3.26E-04	Peroxidase (AHRD V3.3 *** K4BA79_SOLLC)	
Solyc03g098300.1	-2.869952528	1.59E-03	Ornithine decarboxylase 2 (AHRD V3.3 *** A0A060IIA7_ATRBE)	ODC2
Solyc07g008980.3	-2.747255002	1.15E-04	defensin-like protein (AHRD V3.3 *** AT1G19610.1)	
Solyc07g061830.1	-2.643449841	5.12E-03	LOW QUALITY:Sec14p-like phosphatidylinositol transfer family protein (AHRD V3.3 --* AT1G19650.3)	
Solyc06g009610.1	-2.641623077	5.12E-03	LOW QUALITY:GRAS family transcription factor, putative (AHRD V3.3 *** A0A061EWU1_THECC)	
Solyc09g075930.2	-2.62340137	3.69E-03	Amine oxidase (AHRD V3.3 *** K4CVH0_SOLLC)	
Solyc09g014555.1	-2.50738048	7.11E-03	Major latex protein, putative (AHRD V3.3 *** B9T7P8_RICCO)	
Solyc07g053450.3	-2.486702162	1.05E-02	BZIP family transcription factor (AHRD V3.3 *** A0A072VB17_MEDTR)	
Solyc02g070080.3	-2.464082411	2.39E-03	2-oxoglutarate (2OG) and Fe(II)-dependent oxygenase superfamily protein (AHRD V3.3 *** AT4G10500.1)	
Solyc09g011160.3	-2.439307907	1.31E-02	Regulator of chromosome condensation (RCC1) family protein (AHRD V3.3 *** AT3G53830.3)	
Solyc08g005880.3	-2.433032553	2.83E-03	Protein DETOXIFICATION (AHRD V3.3 *** K4CI77_SOLLC)	

Supplemental Table 3. Top 15 uniquely up and down regulated genes for Arachidonic Acid (AA) and Acadian (ANE) treated plants with associated log2 fold change and adjusted P-value data.

	Encysted+Vibrating		Lysis	
Percent ANE	Mean Percent E+V	p-value	Mean Percent Lysis	p-value
0	20.4	0.0267	0.0	1
0.1	27.8	<0.0001	0.0	1
0.2	37.0	<0.0001	1.4	0.9861
0.3	58.6	<0.0001	13.6	0.0012
0.4	66.9	<0.0001	21.0	<0.0001

Supplemental Table 4. Statistical analysis of zoospore motility across timepoints. P-values generated after ANOVA followed by Dunnett's multiple comparisons test of arcsin square root transformed percentage of encysted+vibrating or lysed zoospores compared to corresponding water control.

The oomycete MAMP, arachidonic acid, and an *Ascophyllum nodosum*-derived plant biostimulant induce defense metabolome remodeling in tomato

Domonique C. Lewis[1], Timo van der Zwan[2*], Andrew Richards[2**], Holly Little[2], Gitta L. Coaker[1], and Richard M. Bostock[1†]

[1]Department of Plant Pathology, University of California, Davis, CA 95616, USA

[2]Acadian Plant Health, Acadian Seaplants, Ltd., Dartmouth, Nova Scotia, Canada, B3B 1X8

[†]Corresponding author: R. M. Bostock; E-mail: rmbostock@ucdavis.edu

[*]Current address: Symvivo Corporation, Burnaby, BC, V5J 5J8, Canada

[**]Current address: Department of Plant Pathology, University of California, Davis, CA 95616, USA

Keywords: elicitor, metabolomics, plant immunity, *Solanum lycopersicum*

Funding: Research supported in part by a Gates Millenium Scholars Program fellowship and Jastro-Shields awards to DCL, and an unrestricted gift from Acadian Seaplants, LTD., to RMB.

Abstract

Arachidonic acid (AA) is an oomycete derived MAMP capable of eliciting robust defense responses and inducing resistance in plants. Similarly, extract from the brown seaweed *Ascophylum nodosum*, a plant biostimulant that contains AA, can also prime plants for defense against pathogen challenge. A previous parallel study comparing the transcriptomes of AA and ANE root-treated tomato demonstrated significant overlap in transcriptional profiles, a shared induced resistance phenotype, and changes in accumulation of various defense-related phytohormones. In this work, untargeted metabolomic analysis via LCMS was conducted to investigate the local and systemic metabolome-wide remodeling events elicited by AA- and ANE-root treatment in tomato. Our study demonstrated AA and ANE's capacity to locally and systemically alter the metabolome of tomato with enrichment of chemical classes and accumulation of metabolites associated with defense-related secondary metabolism. AA and ANE root-treated plants showed enrichment of fatty acyl-glycosides and strong modulation of hydroxycinnamic acids and derivatives. Identification of specific metabolites whose accumulation was affected by AA and ANE treatment revealed shared metabolic changes related to ligno-suberin biosynthesis and the synthesis of phenolic compounds. This study highlights the extensive local and systemic metabolic changes in tomato induced by treatment with a fatty acid MAMP and a seaweed-derived plant biostimulant with implications for induced resistance and crop improvement.

Introduction

Plants have pre-formed and inducible structural and biochemical mechanisms to prevent or arrest pathogen ingress and colonization. These defenses include barriers such as papillae and ligno-

suberized layers to fortify cell walls, and low-molecular weight inhibitory chemicals (Freeman and Beattie 2008). Plants undergo transcriptional changes upon perception of microbe associated molecular patterns (MAMPs) or effectors to induce local and systemic resistance.

The oomycete MAMPs, arachidonic acid (AA) and eicosapentaenoic acid (EPA), are potent elicitors of defense. These eicosapolyenoic acids were first identified as active components in *Phytophthora infestans* spore and mycelial extracts capable of eliciting a hypersensitive-like response, phytoalexin accumulation, lignin deposition, and protection against subsequent infection in potato tuber discs (Bostock et al. 1981; Bostock et al. 1982). Further work demonstrated root treatment with AA protects tomato and pepper seedlings from root and crown rot caused by *Phytophthora capsici*, with associated lignification at sites of attempted infection (Dye and Bostock 2021). AA has been shown to induce resistance, elicit production of reactive oxygen species, and trigger programmed cell death in members of the Solanaceae and other families (Araceli et al. 2007; Bostock et al. 1981; Cook et al. 2018; Dedyukhina et al. 2014; Dye et al. 2020; Knight et al. 2001).

Phaeophyta and Rhodophyta members (red and brown macroalgae) contain numerous bioactive chemicals that can elicit defense responses in plants (Klarzynski et al. 2003; Sangha et al. 2010; Vera et al. 2011). The brown alga, *Ascophyllum nodosum*, is a rich source of polyunsaturated fatty acids, including AA and EPA, which comprise nearly 25% of its total fatty acid composition (Lorenzo et al. 2017; van Ginneken et al. 2011). *A. nodosum* and oomycetes belong to the major eukaryotic lineage, the Stramenopila, and share other biochemical features (e.g., both are rich in β-1,3-glucans). Commercial extracts of *A. nodosum*, used in organic and conventional agriculture as plant biostimulants, may also help plants cope with biotic and abiotic stresses. A proprietary *A. nodosum* extract, Acadian (hereafter ANE; APH-1011-00, Acadian

Seaplants, Ltd., Nova Scotia, Canada), has been shown to provide protection against bacterial and fungal pathogens (Ali et al. 2016a). Studies in *A. thaliana* showed ANE induced systemic resistance to *Pseudomonas syringae* pv. *tomato* and *Sclerotinia sclerotiorum* (Subramanian et al. 2011). Investigation into ANE-induced resistance in *A. thaliana* and tomato suggest the role of ROS production, jasmonic acid signaling, and upregulation of defense-related genes and metabolites (Ali et al. 2016b; Cook et al. 2018; Jayaraj et al. 2008; Subramanian et al. 2011). As a predominant polyunsaturated fatty acid in ANE, AA may contribute to ANE's biological activity.

In a parallel study we demonstrated AA's ability to systemically induce resistance and ANE's capacity to locally and systemically induce resistance in tomato to different pathogens (Lewis et al. 2022). Further, we showed that AA and ANE altered the phytohormone profile of tomato by modulating the accumulation of defense-related phytohormones (Lewis et al. 2022). Through RNA sequencing, this same study revealed a striking level of transcriptional overlap in the gene expression profiles of AA- or ANE-root-treated tomato across tested timepoints (Lewis et al. 2022). Gene ontology functional analysis of transcriptomic data revealed AA and ANE enriched similar categories of genes with nearly perfect overlap also observed in categories of under-represented genes. Both AA and ANE treatment protected seedings from challenge with pathogens with different parasitic strategies while eliciting expression of genes involved in immunity and secondary metabolism. The shared induced resistance phenotype and extensive transcriptional overlap of AA and ANE treatments suggested similar metabolic changes may be occurring in treated plants. In the current study, untargeted metabolomic analyses were conducted to assess global effects of root treatment with AA and the AA-containing complex extract, ANE, on the metabolome of tomato plants.

Materials and Methods

Plant growth and root treatment

Plant materials and hydroponic growth system

Seeds of tomato (*Solanum lycopersicum cv.* 'New Yorker') were surface-sterilized and germinated for 10 days on germination paper. Seedlings were transferred to a hydroponic growth system and maintained in a growth chamber as previously described in (Dye et al. 2020). Seed was obtained from a commercial source (Totally Tomatoes, Randolph, WI).

Root treatment and tissue harvest

Fatty acid sodium salts (Na-FA; Nu-Chek Prep, Elysian, MN) were prepared and stored as previously described (Dye et al. 2020). A proprietary formulation of *A. nodosum* extract (ANE; APH-1011-00; Acadian Seaplants, Ltd., Nova Scotia, Canada) was diluted with deionized water (diH2O) to a 10% working concentration, which was used to prepare treatment dilutions. All chemicals were diluted to their treatment concentrations with sterile diH_2O. Hydroponically reared, 3-week-old tomato seedlings with two fully expanded true leaves were transferred to 1 L darkened treatment containers with their respective root treatment solutions. Following 24, 48, 72, and 96 hours of root treatment, tomato seedlings were removed from treatment containers, and leaves and roots were excised from shoots and flash frozen in liquid nitrogen. Each sample was the pool of roots or leaves of two seedlings with four replications per tissue, treatment, and timepoint.

Metabolite extraction

Samples were transported on dry ice and stored at −70 °C until metabolite extraction. Tissue samples were ground in liquid nitrogen using a mortar and pestle and 100 mg was weighed and transferred to a 2-ml bead-beating tube containing four 2.8-mm ceramic beads. All tools and consumables were pre-chilled in liquid nitrogen. After weighing, each sample was removed from liquid nitrogen and kept at −20 °C until addition of extraction solution.

One ml of extraction solution (80 % v/v methanol and 0.1 % v/v formic acid in ultrapure water) was added to each sample which was then vortexed, followed by bead-beating in a bead mill (Bead Mill 24, Fisherbrand) at a speed of 2.9 m/s for one 3-min cycle. After bead-beating, samples were centrifuged at 12k × *g* for 10 min at 4 °C (Accu Spin Micro 17R, Thermo Scientific). Samples were diluted 5-fold using extraction solution and filtered into LCMS-grade HPLC vials using 0.22-µm PTFE syringe filters. HPLC vials were kept at 4 °C until LCMS analysis. A blank was prepared by adding 1 ml extraction solution to a bead-beating tube containing beads that was processed equivalently to the samples. In addition, a quality control sample was prepared by combining 20 µl of each of the extracted samples and processed equivalently.

Liquid chromatography/mass spectrometry run conditions

Samples were analyzed via high performance liquid chromatography (Agilent 1260 Infinity) and electrospray ionization quadrupole time-of-flight mass spectrometry (Agilent 6530 Q-TOF) controlled by MassHunter software in centroid data mode. Mobile phase A was ultrapure water with 0.05 % (v/v) formic acid and mobile phase B was acetonitrile with 0.05 % (v/v) formic acid.

Before starting the run, the column (Poroshell 120 EC-C18; 3.0 mm internal diameter, 50 mm length, 2.7 µm particle size; Agilent), equipped with a guard column (EC-C18; 3.0 mm internal diameter, 5 mm length, 2.7 µm particle size; Agilent), was conditioned for 20 minutes with 95 % mobile phase A and 5 % B. Column temperature was maintained at 40 °C. The sample injection order was randomized, with individual samples being run consecutively in positive and negative mode. The quality control sample was injected at the beginning and end of the run, as well as after every 12 samples throughout the run to check signal and elution stability. Source parameters were as follows: drying gas temperature of 325 °C (positive) and 350 °C (negative), drying gas flow 12 l/min, nebulizer pressure 35 psi, sheath gas temp 375 °C (positive) and 400 °C (negative), sheath gas flow 11 l/min, capillary voltage 3500 V (positive) and 3000 V (negative), nozzle voltage 0 V (positive) and 1500 V (negative), fragmentor 125 V, skimmer 65 V, and octopole 750 V. Acquisition was performed over a mass range of 50 to 1700 m/z using the all-ions MS/MS technique, cycling three different collision energies (0, 10, 30 eV) at an acquisition rate of 3 spectra/s. Simultaneous infusion of a solution of purine and hexakis(1H, 1H, 3H-tetrafluoropropoxy)phosphazine using the reference nebulizer was used throughout the runs for mass calibration. Samples were introduced using 2 µl injections at a flow rate of 0.5 ml/min. A needle wash of 1:1 acetonitrile:water was used between each injection. The mobile phase gradient was: 0 min, 95 % A, 5 % B; 1 min, 95 % A, 5 % B; 10 min, 50 % A, 50 % B; 15 min, 0 % A, 100 % B; 17 min, 0 % A, 100 % B; 17.1 min, 95 % A, 5 % B; 19.1 min, 95 % A, 5 % B.

Data analysis pipeline

Data alignment, deconvolution, and normalization

Positive and negative mode raw data files from MassHunter were analysed separately in MS-DIAL (v. 4.80) before downstream analysis. Tolerances for MS1 and MS2 were set to 0.025 and 0.075 Da respectively (Tsugawa et al. 2015). A representative quality control sample run was used as the reference file to align peaks. For peak detection, the mass slice width was set to 0.1 DA and the minimum peak height was set to 15,000 which was approximately 3 times the noise level observed in the total ion chromatogram. A linear weighted moving average method was used for peak smoothing, with a smoothing level of 3 scans and a minimum peak width of 5 scans. Deconvolution was performed with a sigma window value of 0.5 and an MS/MS abundance cutoff of 10. The adducts permitted were $[M+H]+$, $[M+NH_4]+$, $[M+Na]+$, $[M+K]+$, $[M+H-H_2O]+$, and $[2M+H]+$ in positive mode, and $[M-H]-$, $[M-H_2O-H]-$, $[M+Cl]-$, $[M+Na-2H]-$, and $[M+K-2H]-$ in negative mode.

Quality control, feature annotation, and merging

MS-DIAL data was cleaned in MS-CleanR (*mscleanr*, v. 1.0) in RStudio (v. 1.4.1106) using the following parameters: minimum blank ratio of 0.8, maximum relative standard deviation of 30, minimum relative mass defect (RMD) of 50, maximum RMD of 3000, maximum mass difference of 0.05 and maximum retention time difference of 0.15. MS-DIAL features were clustered by applying a Pearson correlation, with a minimum correlation of 0.8 and maximum p value of 0.05, retaining two features per cluster according to most intense and the most connected peak filters (Fraisier-Vannier et al. 2020). Selected peaks were imported into MS-FINDER (v. 3.52) for annotation (Tsugawa et al. 2016). Mass tolerance for MS1 and MS2 were set to 5 and 15 ppm respectively, the relative abundance cut off set at 1% and the formula finder was configured to use C, H, O, N, P, and S atoms. FooDB, PlantCyc, ChEBI, NPA, NANPDB,

COCONUT, KNApSAcK, PubChem, and UNPD were used as local databases. During the final merge step in MS-CleanR, the best annotation for each peak was based on MS-FINDER scores. The normalized annotated peaks list produced by MS-CleanR was used for the final statistical analyses in R.

Statistical analysis

All statistical analyses were completed in R (v. 4.0.5) via RStudio (v. 1.4.1106). Statistical analyses were run separately for each tissue type using the same parameters.

Multivariate analyses

A partial least squares (PLS) supervised model of the complete log-transformed and Pareto-scaled dataset was done using the *ropls* package (version 1.22.0), with the three treatment groups as the response variables. Ellipses were drawn around treatments using *stat_ellipse* (*ggplot2*) based on a 95 % confidence level. This distance type considers the correlation between variables and the ellipses are created around the centroid data point.

Heatmaps were created using the log-transformed data within the *ComplexHeatmap* package in R (v. 2.13.1), with hierarchical clustering according to the complete-linkage method and Euclidean distance measure across columns and rows, displayed as dendrograms.

Pairwise multivariate analyses

Pairwise multivariate analysis was performed across all time points between ANE and H_2O, and between AA and H_2O, using an orthogonal projections to latent structures discriminant analysis (OPLS-DA). OPLS-DA models were generated using the *ropls* package, with the predictive

components set to 1 and orthogonal components to 7. S-plots were generated following sample sum normalization and Pareto scaling via calculation of p1 (covariance) and pcorr1 (correlation) of the OPLS-DA scores using the *muma* package (v. 1.4) source code within R. Chemical class enrichment analysis was achieved using ChemRICH (version 1.0 August 2020) for each two-treatment comparison at each time point within R using the source code (Barupal and Fiehn 2017). A student's t-test of the signal was conducted to generate p values and effect size. The effect size in each case represents the difference compared to the water control treatment group.

Results

Local and systemic metabolomic analysis of AA- and ANE- induced plants

Previous transcriptomic work revealed a high level of congruency in differentially expressed genes in AA- and ANE-treated tomato seedlings compared to H_2O-treated controls (Lewis et al. 2022). To further this line of investigation, the metabolomic profiles of AA- and ANE-root-treated plants were compared to H_2O after 24-, 48-, 72-, and 96-hours exposure to their respective treatments. Locally-treated roots and distal leaves were harvested, flash frozen, extracted for metabolites, and subsequently analyzed via liquid chromatography/mass spectrometry (**Fig. 1A**).

Partial least squares (PLS) score plots of tomato root tissue revealed distinct clustering by treatment irrespective of timepoint (**Fig. 1C**). No overlap was observed in the 95% confidence ellipses for any treatment group. Likewise, heatmap visualization of the $\log_{10}$ signal of metabolites showed clear clustering of metabolomic profiles by treatment (**Fig. 1B**). Features displayed in the heatmap were filtered from the total dataset with a p-value $< 10^{-6}$ and absolute fold change > 5 in roots.

Less defined clustering was observed in PLS score plots of distal leaf tissue across sampled timepoints (**Fig. 2B**). Ellipses representing the 95% confidence interval for both H_2O and AA treatments both partially overlap with the ANE treatment group. Similarly, a heatmap depicting metabolite log_{10} signal showed more diffuse clustering by treatment (**Fig. 1A**). Visualized metabolites from leaves displayed in the heatmap used a p-value < 0.001 and an absolute fold-change > 2.

Chemical enrichment analysis of AA- and ANE-induced plants

Chemical enrichment analyses were conducted to identify classes of metabolites whose accumulation was locally or systemically altered in AA- and ANE-root-treated tomato seedlings. Enrichment analyses of metabolites whose mean signal was significantly changed in AA- or ANE-treated plants compared to H_2O identified numerous affected chemical classes **(Fig. 3 and Sup. Fig. 1)**. These changes were most robust in directly treated roots compared to distal leaves. Treatment of tomato seedlings with AA showed strong modulation of metabolomic features classified as triterpenoids and linoleic acid and derivatives in roots. AA-treated roots also showed increases in hydroxycinnamic acids and derivatives and fatty acyl glycosides of mono- and disaccharides. ANE-treated roots showed modulation in the accumulation of triterpenoids, steroidal glycosides, and hydroxycinnamic acids and derivatives. Similar to AA-treated plants, the roots of plants treated with ANE also showed increases in metabolites classified as fatty acyl glycosides of mono- and di-saccharides.

Although less striking than the chemical enrichment analysis of roots, leaf tissue of root-treated plants did reveal an altered metabolome **(Sup. Fig. 1)**. These changes in metabolite accumulation occurred most prominently at 96 hours, the latest tested timepoint. Increases in

sesquiterpenoids and steroidal saponins were seen in leaves of AA-treated plants at 96 hours. A mix of accumulation and suppression of terpenoids and an increase of methoxyphenols was observed in the leaves of ANE-root-treated plants.

Specific metabolomic features modulated by AA- and ANE- root treatments

Chemical enrichment analyses broadly revealed classes of metabolites that were induced or suppressed in AA- or ANE-treated plants. To examine which specific variables (metabolites) provide the strongest discriminatory power between the two treatment groups, a two-group comparative supervised multivariate analysis, orthogonal projections to latent structures discriminant analysis (OPLS-DA), was utilized. OPLS-DA score plots show strong between-group variability discrimination between AA and ANE treatment groups compared to the H_2O control across all tested timepoints with the x-axis describing the inter-treatment variability, and the y-axis showing the intra-treatment variability **(Suppl. Figure 2).** S-plots derived from OPLS-DA were examined for both AA and ANE treatments in pairwise comparison with H_2O control. S-plots of OPLS-DA revealed that treatment with AA or ANE induced shared changes in the levels of several defense-related metabolites in roots **(Fig. 4)**. Variables (metabolites) with the most negative and positive correlation and covariance values are the most influential in the model. These metabolites are located on either tail of the S-plot (upper-right and lower-left) and contribute most greatly to the separation between treatment groups

Bar charts depicting mean LCMS signals for top OPLS-DA S-plot metabolites visualized across all timepoints illustrate that AA and ANE have similar effects on plant metabolic response **(Fig. 5)**. Treatment of tomato roots with AA and ANE resulted in a sharp increase in metabolic intermediates in ligno-suberin biosynthesis. This includes AA-induced accumulation of

moupinamide (syn. N-feruloyltyramine) and significant increases in coniferyl alcohol in the roots of ANE-treated plants across all tested timepoints. In roots, AA and ANE treatments also induced increased levels of N-(p-hydroxyphenyl)ethyl p-hydroxycinnamide and N1-trans-feruloylagmatine compared to H_2O treatment, reflecting strong upregulation of the shikimate pathway and phenolic compound synthesis. Reduced levels of tomatine and dehydrotomatine were observed in the roots of AA- and ANE-treated plants indicating suppression of steroid glycoalkaloid biosynthesis. Treated plants also showed lower levels of lyso-phosphatidyl ethanolamine (0:0/18:2(9Z,12Z)) that could reflect enhanced membrane lipid turnover.

Discussion

AA and ANE can induce disease resistance locally and systemically, alter the accumulation of key phytohormones, and change the transcriptional profile of tomato with a striking level of overlap between the two treatments (Lewis et al. 2022). The current study examined and characterized the AA- and ANE-induced metabolomes of tomato. AA and ANE locally and systemically induce metabolome remodeling toward defense-associated metabolic features.

Early studies investigating transcriptional and metabolic changes in potato revealed selective partitioning and shifting of terpenoid biosynthesis from steroidal glycoalkaloids to sesquiterpenes following treatment with AA or EPA or challenged with *P. infestans* (Choi et al. 1992; Stermer and Bostock 1987; Tjamos and Kuć 1982). Similarly, our work here with AA- and ANE-treated tomato seedlings has shown a marked decrease in the levels of two abundant glycoalkaloids, tomatine and dehydrotomatine **(Fig. 5)**. Our data also show strong enrichment of sesquiterpenes in leaves of AA-treated plants at 96 hours post treatment, although the identity of these sesquiterpenes is unresolved **(Sup. Fig. 1A)**. This work further supports evidence for

differential regulation and sub-functionalization of sterol/glycoalkaloid and sesquiterpene biosynthetic pathways in solanaceous plants in different stress contexts (Choi et al. 1992; Stermer and Bostock 1987).

AA and EPA are strong elicitors that are abundant in structural and storage lipids of oomycete pathogens, but absent from higher plants. Although their initial perception by the plant is likely different from that of canonical MAMPs (e.g., flg22, chitosan, lipopolysaccharide), there is some convergence in downstream defenses induced by these various MAMPs. Work to characterize the effect of canonical MAMP treatment on the metabolomes of various plant species has implicated common metabolic changes that prime for defense. Cells and leaf tissue of *A. thaliana* treated with lipopolysaccharide (LPS) showed enrichment of phenylpropanoid pathway metabolites, including cinnamic acid derivatives and glycosides (Finnegan et al. 2016). In the same study, SA and JA were also positively correlated with LPS treatment, as we also observed in tomato following treatment with AA (Finnegan et al. 2016; Lewis et al. 2022). Recent work in *A. thaliana* wild-type and receptor mutants treated with two chemotypes of LPS showed increases in hydroxycinnamic acid and derivatives and enrichment of the associated phenylpropanoid pathway (Offor et al. 2022). Work in tobacco similarly found treatment with LPS, chitosan, and flg22 all induced accumulation of hydroxycinnamic acid and derivatives, and that defense responses elicited by these MAMPs were modulated by both SA and JA (Mhlongo et al. 2016). More recent work in the cells of *Sorghum bicolor* treated with LPS showed enrichment of hydroxycinnamic acids and other phenylpropanoids in coordination with accumulation of both SA and JA (Mareya et al. 2020). Treatment of tomato with flg22 and flgII-28 also enriched hydroxycinnamic acids, and tomato treatment with cps22 revealed a metabolic shift toward the phenylpropanoid pathway with hydroxycinnamic acid, conjugates and

derivatives as key biomarkers (Zeiss et al. 2021a, b). Similar to traditional MAMPs, AA and the AA/EPA-containing complex mixture, ANE, both induce enrichment of cinnamic acid and derivatives in tomato seedlings **(Fig. 3)**. This supports the hypothesis that MAMPs broadly induce similar metabolic changes to enrich pools of specialized secondary metabolites that contribute to plant immunity.

AA- and ANE-treated roots showed strong enrichment of metabolic features classified as fatty acyl glycosides of mono- and disaccharides **(Fig. 3)**. Fatty acyl glycosides have been studied in several plant families and are most extensively characterized in members of Solanaceae (Asai and Fujimoto 2010; Asai et al. 2010; Dalsgaard et al. 2006; Moghe et al. 2017). Investigations into the function of fatty acyl glycosides in plants suggest they may act to protect against insect herbivory through various mechanisms and provide protection against fungal pathogens (Leckie et al. 2016; Luu et al. 2017; Puterka et al. 2003; Simmons et al. 2004; Weinhold and Baldwin 2011). A recent study isolated and identified fatty acyl glycosides from strawberry capable of inducing immune responses in *A. thaliana*, including ROS burst, callose deposition, increased expression of defense-related genes, and induced resistance to bacterial and fungal challenge (Grellet Bournonville et al. 2020). This same work also demonstrated that the strawberry-derived fatty acyl glycosides induced resistance in soybean and, due to their antimicrobial activity, also protected lemon fruits postharvest from fungal infection (Grellet Bournonville et al. 2020). AA- and ANE-root treatments locally elicit accumulation of the same class of defense associated metabolites that Grellet et al. illustrated to have direct antimicrobial activity and protect against disease (Grellet Bournonville et al. 2020).

Cell wall fortification is an important plant defense often initiated upon pathogen infection. Cell wall lignification is a well-studied mechanism with localized accumulation of

phenolic intermediates and lignin at attempted penetration sites (Nicholson and Hammerschmidt 1992; Vance et al. 1980; Zeyen et al. 2002). Lignification reinforces and rigidifies the cell wall to create an impervious barrier to microbial ingress (Nicholson and Hammerschmidt 1992; Vance et al. 1980; Zeyen et al. 2002). In our study, AA treatment of tomato roots induced accumulation of a phenylcoumaran intermediate in lignin biosynthesis, while ANE treatment induced accumulation of coniferyl alcohol, an important monomer unit of lignin. Interestingly, coniferyl alcohol has recently been shown to act in a signaling capacity in a regulatory feedback mechanism to intricately control lignin biosynthesis, an irreversible process that is energetically costly (Guan et al. 2022). The findings of our study coincide with the well-characterized role of lignin and its intermediates in plant defense.

This work characterizes local and systemic metabolic profiles of AA- and ANE-treated tomato with the oomycete-derived MAMP, AA, and the AA-containing biostimulant, ANE. AA and ANE profoundly alter the tomato metabolome toward defense-associated secondary metabolites with notable overlap in enriched metabolite classes compared to H_2O control. Further investigation is required to elucidate the functional contribution of these metabolic features in AA- and ANE induced resistance and, more broadly, plant immunity. Our study adds to the understanding of MAMP-induced metabolomes with implications for further development of seaweed-derived biostimulants for crop improvement.

Author contributions

Study planned by all authors. Experiments performed by DCL, metabolite analyses conducted by TVDZ and AR. Paper written by DCL, TVDZ, and RMB, with editing by GLC and AR.

Literature cited

Ali, N., Farrell, A., Ramsubhag, A., and Jayaraman, J. 2016a. The effect of *Ascophyllum nodosum* extract on the growth, yield and fruit quality of tomato grown under tropical conditions. J. Appl. Phycol. 28:1353-1362.

Ali, N., Ramkissoon, A., Ramsubhag, A., and Jayaraj, J. 2016b. *Ascophyllum* extract application causes reduction of disease levels in field tomatoes grown in a tropical environment. Crop Protect. 83:67-75.

Araceli, A.-C., Elda, C.-M., Edmundo, L.-G., and Ernesto, G.-P. 2007. Capsidiol production in pepper fruits (*Capsicum annuum L.*) induced by arachidonic acid is dependent of an oxidative burst. Physiol. Mol. Plant Pathol. 70:69-76.

Asai, T., and Fujimoto, Y. 2010. Cyclic fatty acyl glycosides in the glandular trichome exudate of *Silene gallica*. Phytochemistry 71:1410-1417.

Asai, T., Hara, N., and Fujimoto, Y. 2010. Fatty acid derivatives and dammarane triterpenes from the glandular trichome exudates of *Ibicella lutea* and *Proboscidea louisiana*. Phytochemistry 71:877-894.

Barupal, D. K., and Fiehn, O. 2017. Chemical Similarity Enrichment Analysis (ChemRICH) as alternative to biochemical pathway mapping for metabolomic datasets. Sci. Rep. 7:14567.

Bostock, R. M., Kuć, J. A., and Laine, R. A. 1981. Eicosapentaenoic and arachidonic acids from *Phytophthora infestans* elicit fungitoxic sesquiterpenes in the potato. Science 212:67-69.

Bostock, R. M., Laine, R. A., and Kuć, J. A. 1982. Factors affecting the elicitation of sesquiterpenoid phytoalexin accumulation by eicosapentaenoic and arachidonic acids in potato. Plant Physiol. 70:1417-1424.

Choi, D., Ward, B. L., and Bostock, R. M. 1992. Differential induction and suppression of potato 3-hydroxy-3-methylglutaryl coenzyme A reductase genes in response to *Phytophthora infestans* and to its elicitor arachidonic acid. Plant Cell 4:1333-1344.

Cook, J., Zhang, J., Norrie, J., Blal, B., and Cheng, Z. 2018. Seaweed extract (Stella Maris(®)) activates innate immune responses in *Arabidopsis thaliana* and protects host against bacterial pathogens. Mar. Drugs 16:221.

Dalsgaard, P. W., Potterat, O., Dieterle, F., Paululat, T., Kühn, T., and Hamburger, M. 2006. Noniosides E - H, new trisaccharide fatty acid esters from the fruit of *Morinda citrifolia* (Noni). Planta Med. 72:1322-1327.

Dedyukhina, E. G., Kamzolova, S. V., and Vainshtein, M. B. 2014. Arachidonic acid as an elicitor of the plant defense response to phytopathogens. Chem. Biol. Technol. 1:18.

Dye, S. M., and Bostock, R. M. 2021. Eicosapolyenoic fatty acids induce defense responses and resistance to *Phytophthora capsici* in tomato and pepper. Physiol. Mol. Plant Pathol. 114:101642.

Dye, S. M., Yang, J., and Bostock, R. M. 2020. Eicosapolyenoic fatty acids alter oxylipin gene expression and fatty acid hydroperoxide profiles in tomato and pepper roots. Physiol. Mol. Plant Pathol. 109:101444.

Finnegan, T., Steenkamp, P. A., Piater, L. A., and Dubery, I. A. 2016. The lipopolysaccharide-induced metabolome signature in *Arabidopsis thaliana* reveals dynamic reprogramming of phytoalexin and phytoanticipin pathways. PLoS One 11:e0163572.

Fraisier-Vannier, O., Chervin, J., Cabanac, G., Puech, V., Fournier, S., Durand, V., Amiel, A., André, O., Benamar, O. A., Dumas, B., Tsugawa, H., and Marti, G. 2020. MS-CleanR: A

feature-filtering workflow for untargeted LC–MS based metabolomics. Anal. Chem. 92:9971-9981.

Freeman, B., and Beattie, G. 2008. An overview of plant defenses against pathogens and herbivores. Plant Health Instr. 149.

Grellet Bournonville, C., Filippone, M. P., Di Peto, P. d. l. Á., Trejo, M. F., Couto, A. S., Mamaní de Marchese, A., Díaz Ricci, J. C., Welin, B., and Castagnaro, A. P. 2020. Strawberry fatty acyl glycosides enhance disease protection, have antibiotic activity and stimulate plant growth. Sci. Rep. 10:8196.

Guan, M., Li, C., Shan, X., Chen, F., Wang, S., Dixon, R. A., and Zhao, Q. 2022. Dual mechanisms of coniferyl alcohol in phenylpropanoid pathway regulation. Front. Plant Sci. 13.

Jayaraj, J., Wan, A., Rahman, M., and Punja, Z. K. 2008. Seaweed extract reduces foliar fungal diseases on carrot. Crop Protect. 27:1360-1366.

Klarzynski, O., Descamps, V., Plesse, B., Yvin, J.-C., Kloareg, B., and Fritig, B. 2003. Sulfated fucan oligosaccharides elicit defense responses in tobacco and local and systemic resistance against Tobacco Mosaic Virus. Mol. Plant-Microbe Interact. 16:115-122.

Knight, V. I., Wang, H., Lincoln, J. E., Lulai, E. C., Gilchrist, D. G., and Bostock, R. M. 2001. Hydroperoxides of fatty acids induce programmed cell death in tomato protoplasts. Physiol. Mol. Plant Pathol. 59:277-286.

Leckie, B. M., D'Ambrosio, D. A., Chappell, T. M., Halitschke, R., De Jong, D. M., Kessler, A., Kennedy, G. G., and Mutschler, M. A. 2016. Differential and synergistic functionality of acylsugars in suppressing oviposition by insect herbivores. PLoS One 11:e0153345.

Lewis, D. C., Stevens, D. M., Little, H., Coaker, G. L., and Bostock, R. M. 2022. Overlapping local and systemic defense induced by an oomycete fatty acid MAMP and brown seaweed extract in tomato.2022.2008.2026.505481.

Lorenzo, J. M., Agregán, R., Munekata, P. E. S., Franco, D., Carballo, J., Şahin, S., Lacomba, R., and Barba, F. J. 2017. Proximate composition and nutritional value of three macroalgae: *Ascophyllum nodosum*, *Fucus vesiculosus* and *Bifurcaria bifurcata*. Mar. Drugs 15:360.

Luu, V. T., Weinhold, A., Ullah, C., Dressel, S., Schoettner, M., Gase, K., Gaquerel, E., Xu, S., and Baldwin, I. T. 2017. O-acyl sugars protect a wild tobacco from both native fungal pathogens and a specialist herbivore. Plant Physiol. 174:370-386.

Mareya, C. R., Tugizimana, F., Di Lorenzo, F., Silipo, A., Piater, L. A., Molinaro, A., and Dubery, I. A. 2020. Adaptive defence-related changes in the metabolome of *Sorghum bicolor* cells in response to lipopolysaccharides of the pathogen *Burkholderia andropogonis*. Sci. Rep. 10:7626.

Mhlongo, M. I., Piater, L. A., Madala, N. E., Steenkamp, P. A., and Dubery, I. A. 2016. Phenylpropanoid defences in *Nicotiana tabacum* cells: overlapping metabolomes indicate common aspects to priming responses induced by lipopolysaccharides, chitosan and flagellin-22. PLoS One 11:e0151350.

Moghe, G. D., Leong, B. J., Hurney, S. M., Daniel Jones, A., and Last, R. L. 2017. Evolutionary routes to biochemical innovation revealed by integrative analysis of a plant-defense related specialized metabolic pathway. ELife 6.

Nicholson, R. L., and Hammerschmidt, R. 1992. Phenolic compounds and their role in disease resistance. Annu. Rev. Phytopathol. 30:369-389.

Offor, B. C., Mhlongo, M. I., Steenkamp, P. A., Dubery, I. A., and Piater, L. A. 2022. Untargeted metabolomics profiling of Arabidopsis WT, *lbr-2-2* and *bak1-4* mutants following treatment with two LPS chemotypes. Metabolites 12.

Puterka, G. J., Farone, W., Palmer, T., and Barrington, A. 2003. Structure-function relationships affecting the insecticidal and miticidal activity of sugar esters. J. Econ. Entomol. 96:636-644.

Sangha, J. S., Ravichandran, S., Prithiviraj, K., Critchley, A. T., and Prithiviraj, B. 2010. Sulfated macroalgal polysaccharides λ-carrageenan and ι-carrageenan differentially alter *Arabidopsis thaliana* resistance to *Sclerotinia sclerotiorum* Physiol. Mol. Plant Pathol. 75:38-45.

Simmons, A. T., Gurr, G. M., McGrath, D., Martin, P. M., and Nicol, H. I. 2004. Entrapment of *Helicoverpa armigera* (Hübner) (Lepidoptera: Noctuidae) on glandular trichomes of *Lycopersicon* species. 43:196-200.

Stermer, B. A., and Bostock, R. M. 1987. Involvement of 3-hydroxy-3-methylglutaryl coenzyme a reductase in the regulation of sesquiterpenoid phytoalexin synthesis in potato. Plant Physiol. 84:404-408.

Subramanian, S., Sangha, J. S., Gray, B. A., Singh, R. P., Hiltz, D., Critchley, A. T., and Prithiviraj, B. 2011. Extracts of the marine brown macroalga, *Ascophyllum nodosum*, induce jasmonic acid dependent systemic resistance in *Arabidopsis thaliana* against *Pseudomonas syringae pv. tomato* DC3000 and *Sclerotinia sclerotiorum*. Eur. J. Plant Pathol. 131:237-248.

Tjamos, E. C., and Kuć, J. A. 1982. Inhibition of steroid glycoalkaloid accumulation by arachidonic and eicosapentaenoic acids in potato. Science 217:542-544.

Tsugawa, H., Kind, T., Nakabayashi, R., Yukihira, D., Tanaka, W., Cajka, T., Saito, K., Fiehn, O., and Arita, M. 2016. Hydrogen rearrangement rules: computational MS/MS fragmentation and structure elucidation using MS-FINDER software. Anal. Chem. 88:7946-7958.

Tsugawa, H., Cajka, T., Kind, T., Ma, Y., Higgins, B., Ikeda, K., Kanazawa, M., VanderGheynst, J., Fiehn, O., and Arita, M. 2015. MS-DIAL: data-independent MS/MS deconvolution for comprehensive metabolome analysis. Nat. Methods 12:523-526.

van Ginneken, V. J., Helsper, J. P., de Visser, W., van Keulen, H., and Brandenburg, W. A. 2011. Polyunsaturated fatty acids in various macroalgal species from North Atlantic and tropical seas. Lipids Health Dis 10:104.

Vance, C., Kirk, T., and Sherwood, R. 1980. Lignification as a mechanism of disease resistance. Annu. Rev. Phytopathol. 18:259-288.

Vera, J., Castro, J., Gonzalez, A., and Moenne, A. 2011. Seaweed polysaccharides and derived oligosaccharides stimulate defense responses and protection against pathogens in plants. Mar. Drugs 9:2514-2525.

Weinhold, A., and Baldwin, I. T. 2011. Trichome-derived O-acyl sugars are a first meal for caterpillars that tags them for predation. PNAS 108:7855-7859.

Zeiss, D. R., Steenkamp, P. A., Piater, L. A., and Dubery, I. A. 2021a. Altered metabolomic states elicited by Flg22 and FlgII-28 in *Solanum lycopersicum*: intracellular perturbations and metabolite defenses. BMC Plant Biol. 21:429.

Zeiss, D. R., Steenkamp, P. A., Piater, L. A., and Dubery, I. A. 2021b. Metabolomic Evaluation of *Ralstonia solanacearum* Cold Shock Protein Peptide (csp22)-Induced Responses in *Solanum lycopersicum*. Front. Plant Sci. 12:803104.

Zeyen, R., Carver, T., and Lyngkjaer, M. 2002. Epidermal cell papillae In: Belanger R R, Bushnell WR (ed) The powdery mildew: a comprehensive treatise. APS Press, MN, USA.

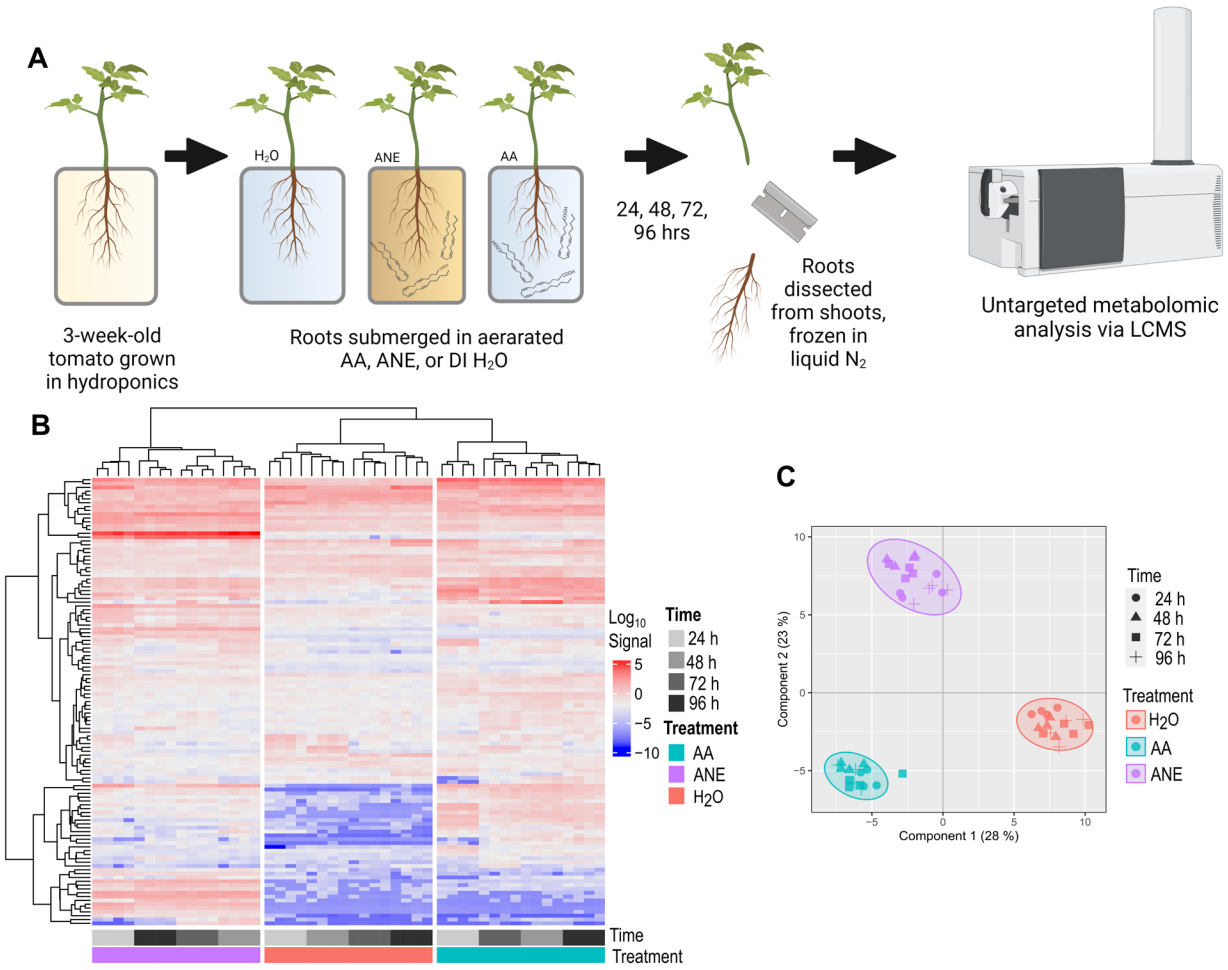

Figure 1. (A) Experimental procedure for the untargeted metabolomics study. Tomato roots were treated with 10 µM AA, 0.4% ANE, or H_2O. Following 24, 48, 72, and 96 hours of root exposure to their respective treatments, plants were harvested, root and leaf tissue dissected from shoots, and the collected tissue flash frozen in liquid nitrogen. Harvested tissue was then subjected to metabolite extraction and liquid chromatography/mass spectrometry. **(B)** Log10 signal of metabolites from root tissue of 10 µM AA-, 0.4% ANE-, or H_2O-treated plants sampled at 24, 48, 72, and 96 hours or treatment. Features visualized in the heatmap are filtered from the total dataset having an adjusted p-value < 10^{-6} and a fold change > 5. Heatmap data is log10 transformed and hierarchical clustering was conducted across rows and columns. **(C)** Partial least squares score plots of tomato root metabolites after 24, 48, 72, and 96 hours of treatment

with 10 μM AA, 0.4% ANE, or H_2O. Ellipses indicate the 95% confidence intervals. Score plots show variance of 4 biological replicates performed per timepoint and treatment.

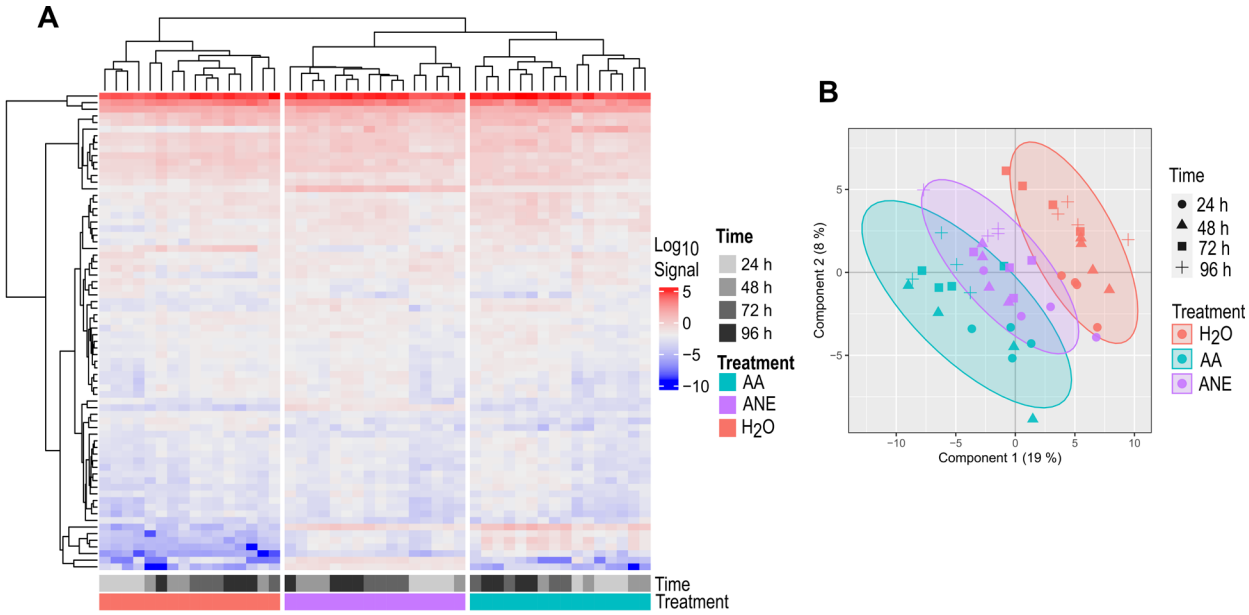

Figure 2. (A) Log10 signal of metabolites from leaf tissue of 10 µM AA-, 0.4% ANE-, or H_2O-treated plants at 24, 48, 72, and 96 hours of treatment. Features visualized in the heatmap are filtered from the total dataset having an adjusted p-value < 0.001 and a fold change > 2. Heatmap data is log10 transformed and heirachical clustering was conducted across rows and columns. **(B)** Partial least squares score plots of tomato leaf metabolites after 24,48, 72, and 96 hours of treatment with 10 µM AA, 0.4% ANE, or H_2O. Score plots show variance of 4 biological replicates performed per timepoint and treatment. Ellipses indicate the 95% confidence intervals.

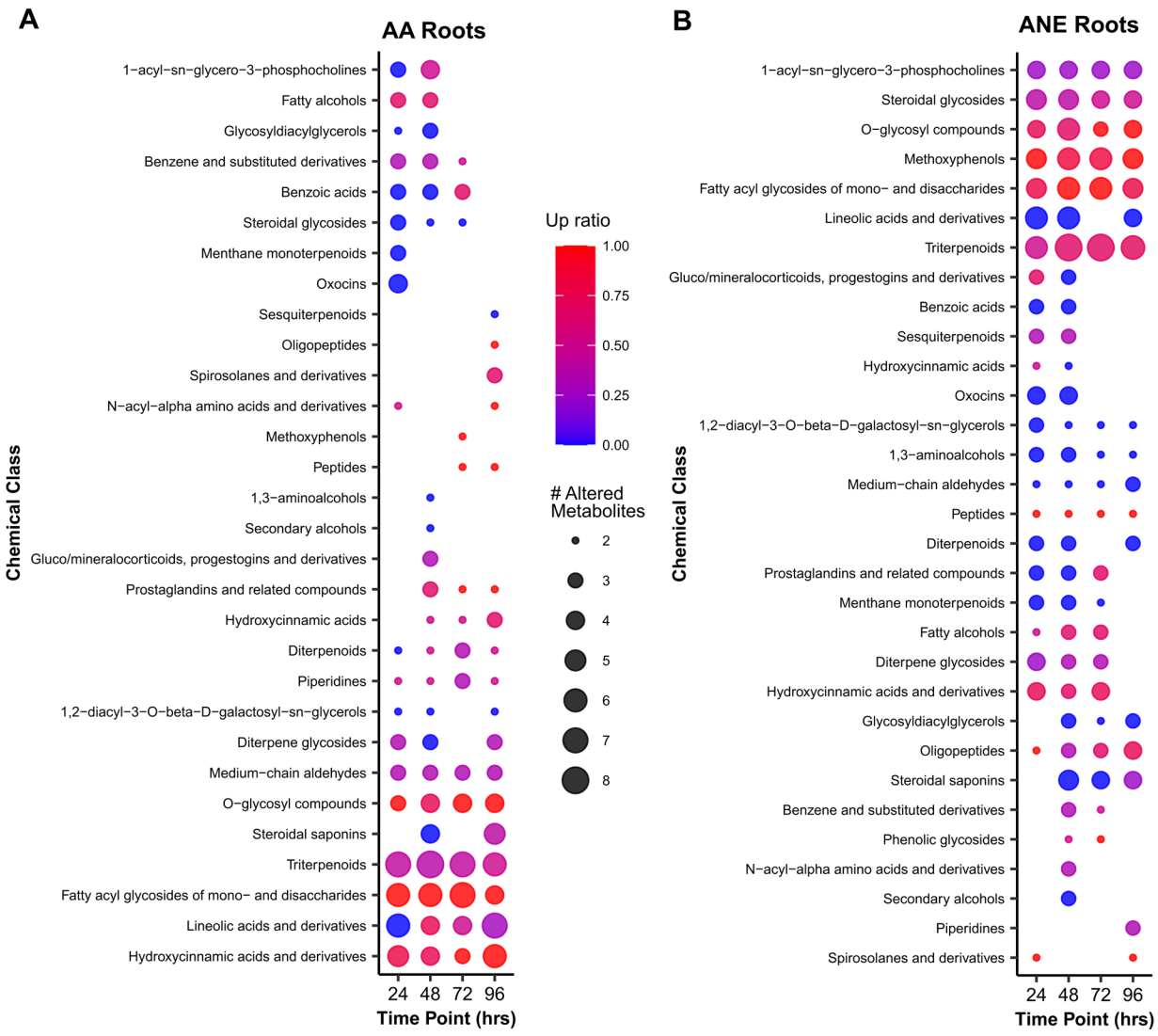

Figure 3. Dot plot illustrating chemical enrichment analysis of significantly altered metabolite clusters in roots of **(A)** AA- and **(B)** ANE-root-treated plants compared to H_2O after 24, 48, 72, 96 hours of treatment. Dot sizes indicate the number of altered metabolites per identified cluster. Dot color scale indicates the ratio of up (red) and down (blue) compounds in AA- and ANE-treated plants compared to H_2O. Up ratio represents the proportion of increased/decreased metabolites compared to H_2O.

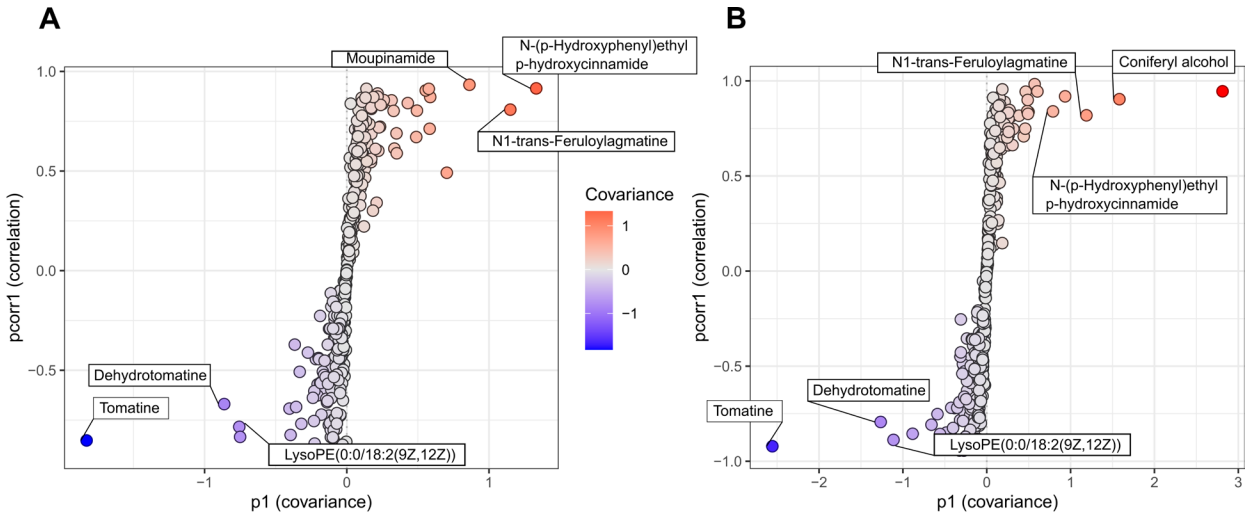

Figure 4. S-plots derived from orthogonal projections to latent structures discriminant analysis (O-PLS-DA) models for the roots of **(A)** AA-treated and **(B)** ANE-treated plants in pairwise comparison with H_2O across all tested timepoints. Color scale represents covariance strength and direction with red data points indicating most positive covariance and blue indicating most negative covariance.

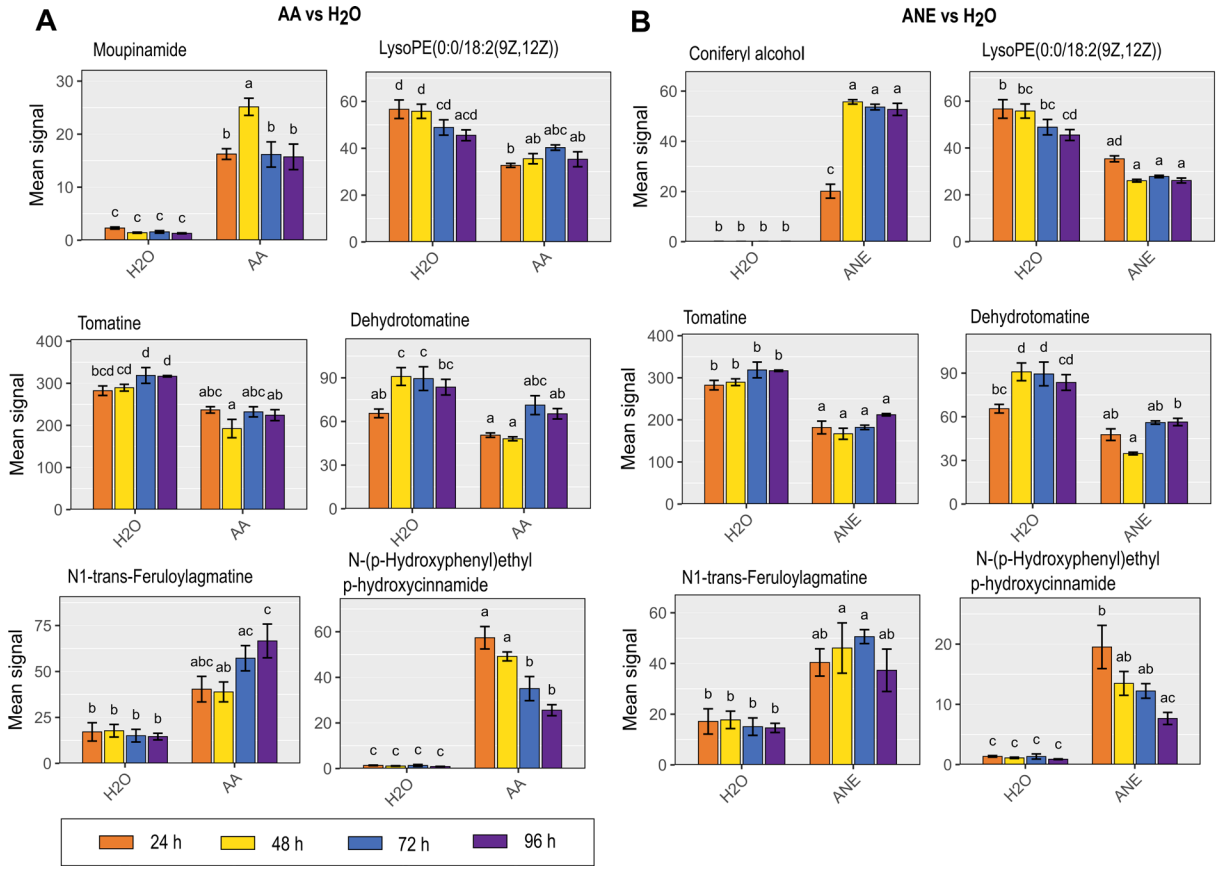

Figure 5. Mean LCMS signals for the top O-PLS-DA S-plot metabolites visualized across 24, 48, 72, and 96 hour timepoints for **(A)** AA- and **(B)** ANE-treated roots in pairwise comparison with H_2O.

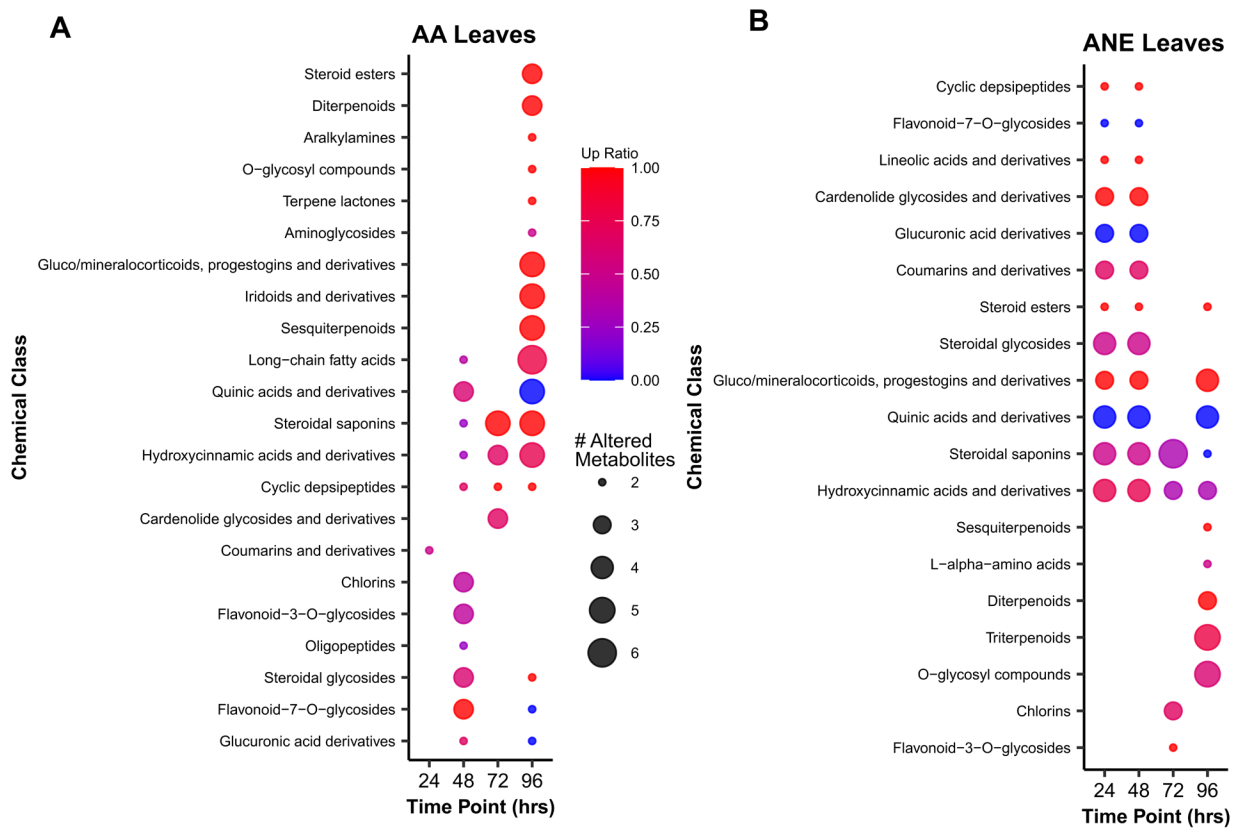

Supplemental Figure 1. Chemical enrichment analysis of significantly altered metabolite clusters in leaves of **(A)** AA- and **(B)** ANE-root-treated plants compared to H_2O after 24, 48, 72, 96 hours of treatment. Point sizes indicate the number of altered metabolites per identified cluster. Point color scale indicates the ratio of up (red) and down (blue) compounds in AA- and ANE-treated plants compared to H_2O. Up ratio represents the proportion of increased/decreased metabolites compared to H_2O.

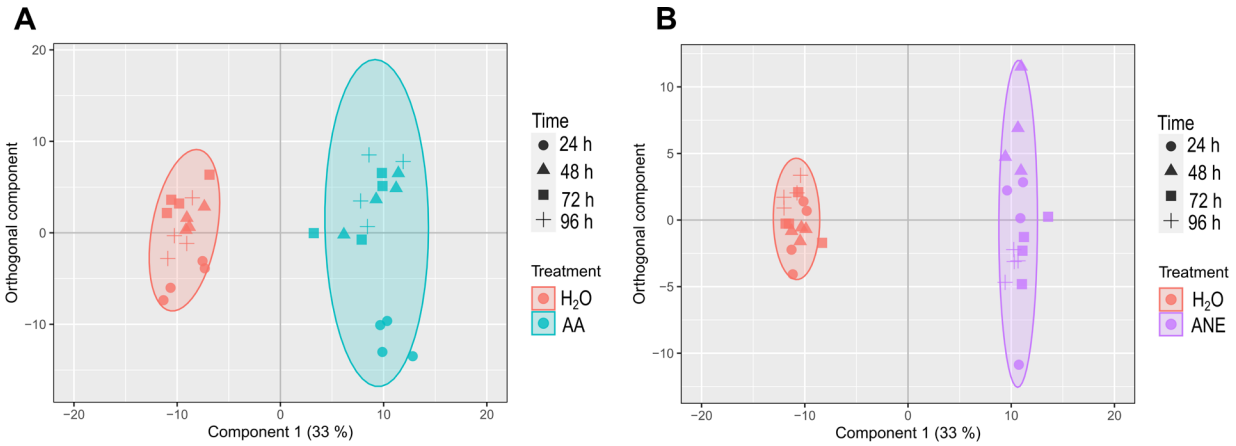

Supplemental Figure 2. Orthogonal projections to latent discriminant analysis score plots of tomato root metabolites after 24, 48, 72, and 96 hours of treatment with (A) 10 µM AA and (B) 0.4% ANE in pairwise comparison to H_2O. Ellipses indicate the 95% confidence intervals. Score plots show represent 4 biological replicates performed per timepoint and treatment.

Appendix – Future Directions

The RNA sequencing analysis reported in this dissertation and other previous studies implicate a role of oxylipin genes in AA- and ANE-induced resistance. The endogenous 9-LOX and 13-LOX oxylipin pathways offer a unique way for AA and, by inference, ANE to engage jasmonic acid (JA) and immune signaling. Although Savchenko et al. demonstrated that *A. thaliana aos* mutants showed no AA-induced resistance to *B. cinerea*, to date there has been no definitive functional analysis performed on identified oxylipin genes and their contribution to AA- or ANE-induced resistance in solanaceous hosts.

To further the work of this dissertation, a premiere genome editing tool such as CRISPR/Cas9 could be used to edit oxylipin candidate genes in tomato. Possible CRISPR/Cas9 gene targets in this pathway include 9-lipoxygenase (9-LOX), α-dioxygenase (α-DOX), and 9-divinyl ether synthase (9-DES). The action of LOXs or α-DOX represent a first step in the generation of plant oxylipins with the production of hydroperoxy and α-hydroperoxy fatty acids respectively. 9-DES produces important antimicrobial divinyl ethers from fatty acid hydroperoxide products of LOX action. Using CRISPR/Cas9 genome editing, these genes could be removed from tomato in 3 separate lines with subsequent disease resistance phenotyping to assess the effects of each gene on AA- and ANE-induced resistance. I began work on this objective by designing appropriate guide RNAs and generating the necessary plasmid constructs. Additional work remains to successfully introduce the DNA constructs into competent DH5α *E. coli* for amplification and subsequent introduction into *A. tumefaciens* for use in producing the CRISP/Cas9 edited tomato lines.

Other critical work that remains is characterizing the chemical composition of ANE. ANE is a complex mixture containing EPs, however the concentrations of free and esterified AA and EPA are not known. Likewise, the presence and concentrations of β-1,3-glucans and other bioactive compounds that may contribute to ANE elicitor activity is not established. It would also be relevant to conduct fractionation experiments to determine the individual constituents that contribute to observed induced resistance phenotypes. Identifying and characterizing the biologically active components of ANE would facilitate better deployment and utilization of seaweed-based biostimulants for disease control.

Further metabolomics studies could be conducted to investigate and possibly identify novel oxylipins of AA. It is important to note that pepper, potato, and tobacco 9-LOXs can use AA as a substrate to produce various fatty acid hydroperoxides. However, there are likely unique products that have yet to be identified that could potentially act in a signaling capacity. Similarly, there are unknown potential AA-derived products of 9-DES whose structure and activity should be investigated. Additional study into novel products of oxylipin-producing enzymes would aid understanding of plant immune signaling and induced resistance.